We are IntechOpen, the world's leading publisher of Open Access books
Built by scientists, for scientists

5,900
Open access books available

145,000
International authors and editors

180M
Downloads

Our authors are among the

154
Countries delivered to

TOP 1%
most cited scientists

12.2%
Contributors from top 500 universities

CLARIVATE ANALYTICS
BOOK CITATION INDEX
INDEXED

WEB OF SCIENCE™

Selection of our books indexed in the Book Citation Index
in Web of Science™ Core Collection (BKCI)

Interested in publishing with us?
Contact book.department@intechopen.com

Numbers displayed above are based on latest data collected.
For more information visit www.intechopen.com

Creep Lifing Models and Techniques

Zakaria Abdallah, Karen Perkins and Cris Arnold

Additional information is available at the end of the chapter

Abstract

The deformation of structural alloys presents problems for power plants and aerospace applications due to the demand for elevated temperatures for higher efficiencies and reductions in greenhouse gas emissions. The materials used in such applications experience harsh environments which may lead to deformation and failure of critical components. To avoid such catastrophic failures and also increase efficiency, future designs must utilise novel/improved alloy systems with enhanced temperature capability. In recognising this issue, a detailed understanding of creep is essential for the success of these designs by ensuring components that do not experience excessive deformation which may ultimately lead to failure. To achieve this, a variety of parametric methods have been developed to quantify creep and creep fracture in high temperature applications. This study reviews a number of well-known traditionally employed creep lifing methods with some more recent approaches also included. The first section of this paper focuses on predicting the long-term creep-rupture properties which is an area of interest for the power generation sector. The second section looks at pre-defined strains and the re-production of full creep curves based on available data which is pertinent to the aerospace industry where components are replaced before failure.

Keywords: creep, creep lifing methods, long-term creep behaviour, stress rupture, creep prediction

1. Introduction

The drive towards more efficient gas turbines and the associated reductions in greenhouse emissions require the existing gas turbines to operate under higher severe temperatures. However, this aim is restricted by the limitation of the materials used in such harsh environments which may, eventually, lead to the deformation and failure of these components. In order to avoid such catastrophic failures and increase the efficiency, future designs must utilise

novel or improved alloy systems with an enhanced temperature capability. One key material property that governs the life of many components within the gas turbine is creep. A detailed understanding of the creep behaviour of materials is seen as an essential requirement. However, understanding and predicting the creep properties is a very important challenge for researchers, which is the basis of this chapter. Therefore, the current research will thoroughly concentrate and investigate the long-term creep predictions of materials as well as their behavioural attributes under the applied stresses and temperatures.

Creep is defined as the plastic deformation of materials under the effect of high stresses and temperatures for long durations of time which, eventually, leads to fracture. Generally speaking, problems of creep failure and excessive distortion are experienced at temperatures equal, or just above, to the half of the melting temperature, TM, of a material. It might be possible to avoid creep problems by either selecting materials of high melting temperatures or maintaining the operation temperatures far away from those at which creep could take place, typically less than the third of the melting point of a material. However, these simple solutions do not provide a comprehensive and convincing answer to the problem. On one hand, materials of high melting temperatures can be developed and employed but will still show creep deformation under the high stresses and temperatures encountered in such applications. On the other hand, if temperatures are lowered to less than the third of the melting temperature, this will, in return, lower the efficiency, which is undesirable in these applications. Therefore, the design stage is the crucial part of the industrial process where decisions should be taken so as to avoid the long-term creep failures [1].

During the design stage, a comprehensive study and analysis of a material's behaviour should be made before this material is considered for a particular application. For certain applications, this might be adequate but for fundamental studies of creep behaviour, full creep curves must be available. For this purpose, creep tests can be carried out at different stresses and temperatures in order to provide the designer with the necessary information to study and analyse the long-term behaviour of materials under the applied stresses and temperatures. Since it is impractical to perform creep tests for the entire lifetime of some real applications, particularly when lifetimes can range, for instance, from 20,000 to 120,000 h as in the power generation applications, determining a conservative and an acceptable method for extrapolating the short-term measurements is a significant goal. Alternatively, for aerospace applications, where the time to a certain percentage strain is more desirable, this method should also provide accurate predictions of the creep behaviour based on this criterion. Starting from this point, many extrapolation techniques were devised for the purpose of predicting the long-term creep behaviour of materials without the need to carry out practical tests which could last for many years before being able to size and manufacture the required components. Minimising the scale of these larger tests will, in return, reduce the cost and save the time needed for such long-term tests. Hence, these predictions require short-term data to be available from the various types of creep tests at the same conditions as the actual application. Extrapolation methods must be taken into consideration that creep is a critical function of stress and temperature, that is, a relatively small change in either of these quantities can drastically affect the material's lifetime. These methods are being used to predict both creep-rupture and creep-deformation behaviours, in which the former has received a greater attention than the latter as a result of the more drastic consequences of brittle failures, that is, sudden rupture, compared with ductile failures, that is, excess deformation [2].

2. Review of creep parametric methods

Many approaches were proposed in an effort to predict the long-term creep properties based on short-term creep measurements so as to reduce the time scales and costs required to obtain such long-term data. Each of these approaches represents a technique through which the short-term creep-rupture data can be extrapolated using a time-temperature parameter. This concept is based on the assumption that all creep-rupture data, for a given material, can be superimposed to produce a single 'master curve' wherein the stress is plotted against a parameter that contains and combines time and temperature. Based on this master curve, that can only be constructed using available short-term measurements; extrapolation to longer times can then be obtained. These parametric methods play a key role during the design stage in which the high temperature components are designed to codes that are intended to assure a specific life. Generally, these design codes define a maximum allowable stress that can exist in a component during the anticipated design life. This allowable design stress, which is a combined function of time, temperature and material, is usually based on the rupture stress required to give the expected design life. It is tempting to infer that the plant will give a satisfactory service up to, but not much beyond, the design life. For this reason, two distinct parts of the service life can be defined, namely: (a) the original design life which can typically be 100,000 h and (b) the safe economic life. Although the latter is normally outside the influence of the design codes, it can be considered as a significant fraction of the overall service life. Moreover, due to the time-dependent nature of materials' properties at high temperatures and the fact that ultimate failure is, thus, implicit, consideration must be always given to a 'beyond design' end-of-life criterion. Since the time required for a crack to grow can be very short, life extension is only safe within the time scale for crack initiation unless defect growth is being monitored [3].

In general, current methods normally involve two approaches, namely: (1) those which involve the acquisition and monitoring of operational parameters, the use of standard materials data and the life fraction rule and (2) those based on post-service examination and testing which require direct access to the component being examined for sampling and measurement [3]. These parametric methods have a great advantage, at least in theory, of requiring only a relatively small amount of data to establish the required master curve. Some of these approaches proved their validity for creep predictions by providing satisfactory results whereas others failed to give precise long-term predictions.

2.1. Review of the power law

The power law represents a combination of the temperature and stress dependences of creep rate which are described by, respectively, Arrhenius's and Norton's laws. In these two laws, the secondary strain rate, $\acute{\varepsilon}_s$, is used to describe the creep rate of materials, as follows [1]:

- **Arrhenius Law:** As the strain rate, $\acute{\varepsilon}_s$, increases with increasing the temperature, T, a straight line relationship can be obtained when plotting (ln $\acute{\varepsilon}_s$) against (1/T), as shown in **Figure 1(a)**. Thus;

$$\acute{\varepsilon}_s \ \alpha \ \exp\left(-Qc/RT\right) \qquad (1)$$

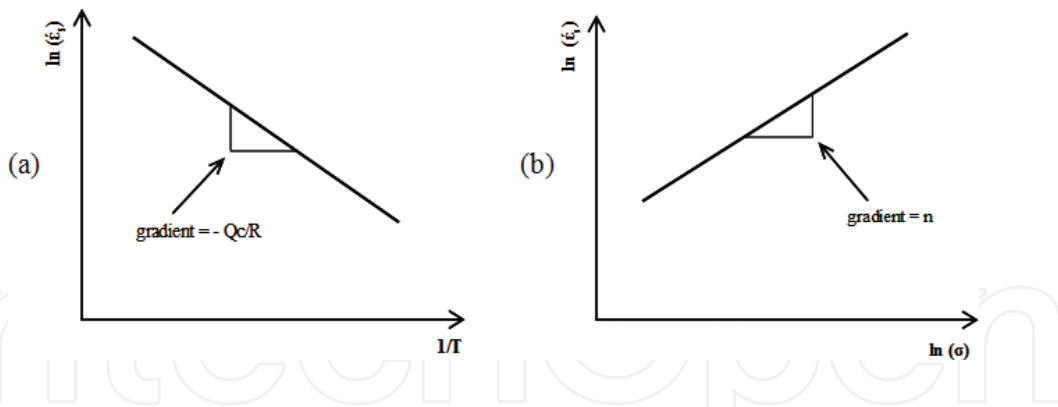where Qc is the activation energy for creep and R is the gas constant.

Figure 1. The secondary creep rate dependence of (a) temperature and (b) stress, respectively.

- **Norton's Law:** As the strain rate, $\acute{\varepsilon}_s$, increases with increasing the stress, σ, another straight line relationship can be obtained when plotting ($\ln \acute{\varepsilon}_s$) against ($\ln \sigma$), as shown in **Figure 1(b)**. Thus;

$$\acute{\varepsilon}_s \, \alpha \, \sigma^n \tag{2}$$

where n is the stress exponent. Combining these two laws together, that is, Eqs. (1) and (2), gives the power law equation as [1]:

$$\acute{\varepsilon}_s = A \, \sigma^n \exp\left(-Qc/RT\right) \tag{3}$$

where A is a constant.

It was also assumed that the value of Qc and n is constant but, in fact, after further research, it was found that their values vary according to the creep mechanism in different stress and temperature regimes [4]. The value of Qc is related to temperature, according to Eq. (1) and **Figure 2(a)**, such that Q_1 and Q_2 represent the value of Qc at high temperatures (due to vacancy flow through the lattice) and low temperatures (due to vacancy flow along grain boundaries), respectively [1]. On the other hand, the value of n is related to stress, according to Eq. (2) and **Figure 2(b)**, such that n_1 and n_2 represent the value of n at high stresses (due to dislocation creep) and low stresses (due to diffusional creep), respectively [1].
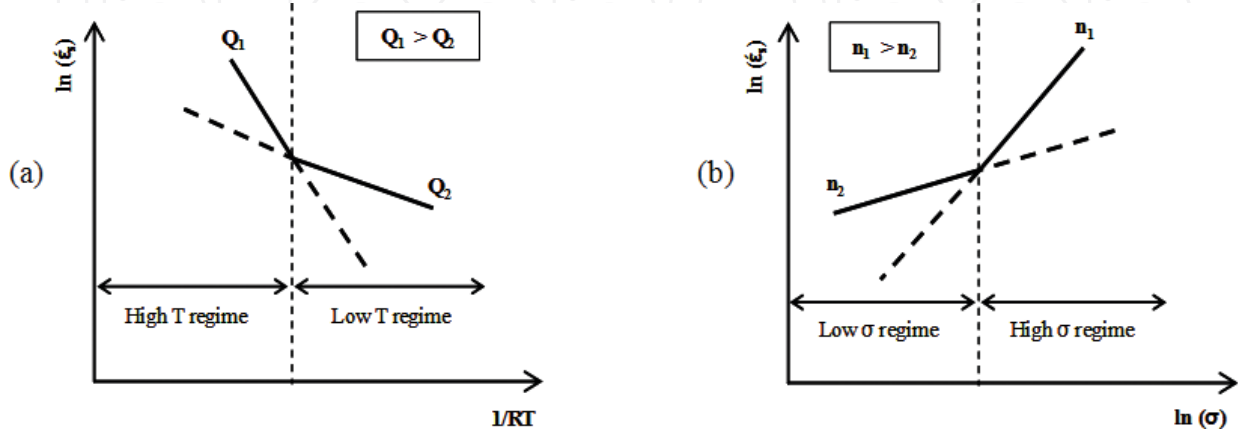

Figure 2. Transition of (a) Qc and (b) n, relative to temperature and stress, respectively.

According to Wilshire and Scharning [5, 6], when creep tests were carried out on the 9–12% chromium steels, it was found that the value of Qc and n was changing with increasing the temperature and decreasing the stress. Therefore, it can be deduced that there is a variation in the value of Qc and n used in the power law equation depending, respectively, on temperature and stress regimes during the creep process. For this reason, and since these values vary in an unpredictable manner, the power law equation does not allow accurate estimation of the long-term rupture strengths by extrapolating the short-term measurements [5, 6]. Furthermore, using these relationships for extrapolation will overestimate the actual long-term performance, **Figure 3**, which might lead to considerable errors in the prediction of creep behaviour and thus, catastrophic consequences. If a certain method is unable to accurately predict the creep behaviour, the consequences will be less severe if the method underestimates the actual measurements rather than overestimating them, as underestimation will keep the component life within the safe operational conditions.

2.2. Review of the Larson-Miller (LM) methodology

This parametric approach is one of the methods used to predict the stress rupture data of metals. It has been originally derived from Arrhenius relation at a constant stress and thus, a constant stress exponent n, but at a variable value of T and Qc, which gave the final form of this relation as [7]:

$$P_{LM} = f(\sigma) = T(C_{LM} + \log t_f) \tag{4}$$

where C_{LM} and P_{LM} are the Larson-Miller constant and parameter, respectively. The parameter, P_{LM}, can be used to superimpose the family of rupture curves into a single master curve [2]. The constant, C_{LM}, includes the Monkman-Grant constant M [8], which is a function of Qc that was proved elsewhere [2, 5, 6] to be a function of stress. Plotting $\log t_f$ against $1/T$ at constant
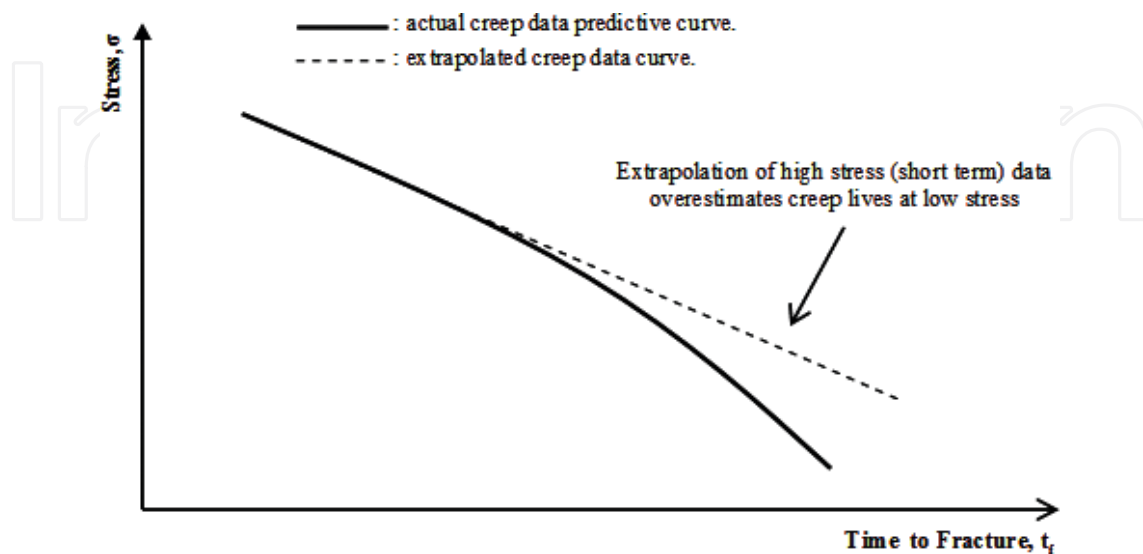

Figure 3. Extrapolation using the power law overestimates actual results.
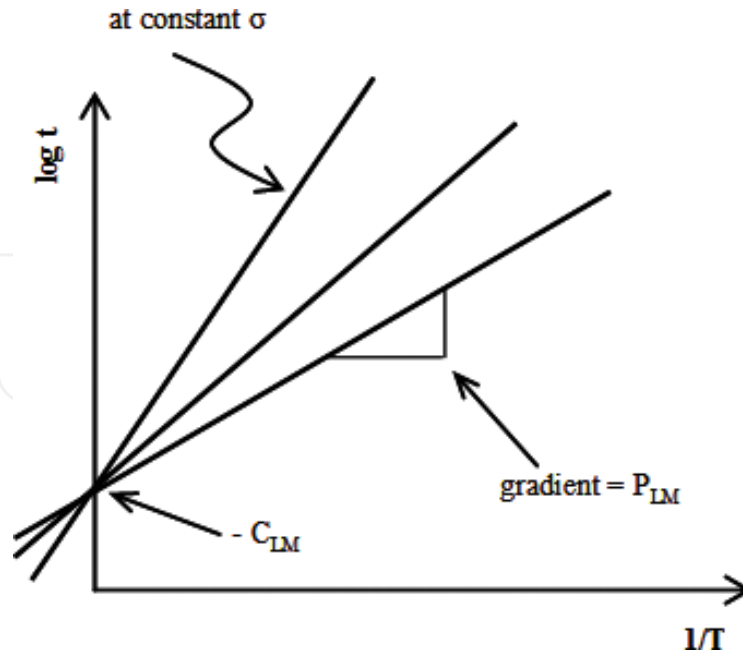
Figure 4. Determination of the Larson-Miller constant.

stresses, **Figure 4**, for some experimental data gave straight lines of slope P_{LM} and an intercept of - C_{LM} [9].

This method was further studied by Krivenyuk and Mamuzic [10], who described the constant C_{LM}, as:

$$C_{LM} = (T/\Delta T)\ m'\ \log\ (\sigma_1/\sigma_2) \tag{5}$$

where σ_1 and σ_2 are the corresponding stresses at a constant time value from two rectilinear stress rupture (SR) curves tested at T_1 and T_2 (where $T_2 = T_1 + \Delta T$), and m' is the reciprocal of the slope, at the selected time value, of the SR curve at temperature T_1. When the value of C_{LM} was estimated based on the data of two rectilinear SR curves at temperature T_1 and T_2, it was found that the value of C_{LM} depends on the position of the two curves relative to each other. In other words, if the curves were parallel then, this means that, C_{LM} is constant. But, if the slope changed from one curve to another then, as the time to rupture increases, the value of the logarithm in Eq. (5) also increases leading to a significant dependence of C_{LM} on time. Hence, for equidistant curves, the time dependence of the constant C_{LM} is weak, whereas it might become sharp for curves that are distinguished by their slopes [10].

Larson and Miller took one step further in their original proposal, suggesting that the value of the constant C_{LM} could be taken as 20 for many metallic materials [7, 11]. However, it was found that the value of this constant varies from one alloy to another and is also influenced by factors such as cold-working, thermo-mechanical processing, phase transitions and/or other structural modifications [11]. Moreover, most applications of the Larson-Miller parameter are made by first calculating the value of C_{LM} that provides the best fit of the raw data, which means that C_{LM} is treated as a 'fitting constant' based on a 'trial and error' method instead of

being a physically meaningful constant. For instance, a certain study [11] showed that the value of this constant for specific aluminium alloys ranged from about 13 to 27.

In studies of refractory and heat-resistant steels and alloys by Krivenyuk and Mamuzic [10], calculations often gave rather lower values of the constant C_{LM} than the commonly used value of 20. In these investigations, the difference in the values of this constant was mainly a result of the time dependence of this constant. In addition, the refractory metals were primarily studied at short loading times whereas the heat-resistant materials were investigated at longer loading times which led to higher values of C_{LM} for the latter, according to formula (5). In agreement with these findings, Cipolla and Gabrel [12] found a huge stress overestimation when the Larson-Miller equation was used on the high chromium steel (Grade 91) at all temperatures, especially at 600°C. Therefore, the requirement of a physical realism of extrapolation was not completely fulfilled by this method which is less conservative and seems to be less able to describe the strong curvature between the low and the high stress regimes.

The equation of Larson and Miller was reviewed by Wilshire and Scharning [5, 6] on the 9–12% chromium steels. Although it was generally accepted that C_{LM} should be taken as 20, the data fit with the curving LM plots was, frequently, better with other values, where, in the case of chromium steels, the best fit was obtained when C_{LM} was 36 instead of 20. This difference in the value of C_{LM} was attributed to the fact that it is a function of Qc which is, itself, a 'variable'. Thus, Larson and Miller's results were only in agreement with the theoretical equation for low temperature deformation, and could not accurately describe the high temperature properties.

A very logical explanation was given by Larke and Inglis [13] who assumed that if two different materials were tested at the same temperature, T, and fractured at the same time, t_f, then if the value of C_{LM} was the same for both materials, Eq. (4) would give the same value for P_{LM}, even though, as would in general be so, the stress to cause fracture is different for each material. Therefore, if the value of C_{LM} is considered 'presumably' as 20, as Larson and Miller suggested, then this suggestion will imply that, for the same conditions of testing, the fracture time would be the same for all materials, which is apparently unacceptable. In addition, this suggestion also means that if, for a given material, a set of stress rupture curves at different temperatures are established, then, over the same temperature range, these curves would be valid for any other material provided that only the stress scale is altered [13].

The graphical method, **Figure 4** recommended by Larson and Miller for determining the numerical value of C_{LM} was proved to be quite unsatisfactory [13]. This was based on the fact that, at least, one pair of lines intersects at a significantly different value of log t_f than the other pairs, and this, coupled with the fact that personal choice enters into the drawing of the curves associated with the basic log σ/log t_f data, increases the doubts on the acceptability of this method for determining the value of C_{LM} [13]. Another critical assessment of this method documented in Murry [14] concluded that the different curves which represent the variations of the Larson-Miller parameter with the initial stress, at different temperatures, very rarely coincided. It was also observed that the value of C_{LM} could vary from 2 to 55, very often in relation to the initial stress. In agreement with this assessment, another study also documented in Murry [14] found that the constant C_{LM} varied with the material, the test temperature and the initial stress. Along with these studies, another extensive work carried out by Penny

and Marriott [2] on the Larson-Miller method stated that this method stands alone as the least accurate of all methods, both in correlation and extrapolation, where errors resulting from its use are significant even when good quality data are available.

Therefore, this parametric formula could only be used to a very limited extent to extrapolate time, temperature, stress and elongation since the value of C_{LM} was found to be variable. Moreover, the unknown curvature of the parametric plots of the Larson-Miller equation makes data extrapolation unreliable. Hence, even when tests lasting up to 30,000 h have been completed, this parametric method does not allow unambiguous determination of the 100,000 h rupture strengths.

2.3. Review of the Manson-Haferd (MH) methodology

Manson and Haferd [15] developed a linear time-temperature relationship for extrapolating creep and stress rupture data. The Manson-Haferd (MH) methodology was developed in order to eliminate the errors introduced by the Larson-Miller technique which assumed a fixed value of the constant used in its equation that led to inaccuracies in predicting the creep life [2, 15]. This technique assumes the same starting point of steady-state creep dominated by a power law behaviour but considers, later on, that the logarithm of the time varies linearly with the test temperature at a constant initial stress, according to [14, 15]:

$$\log t = a - P_{MH}\, T \qquad (6)$$

where t is the time (either the time to fracture, t_f, or to a certain strain level, t_ε), a = $\log t_a$ + P_{MH} T_a (where t_a, P_{MH} and T_a are the Manson-Haferd time, parameter, and temperature constants, respectively), T is the absolute creep test temperature, and the point (T_a, t_a) is the point of intersection of the straight lines corresponding to the various iso-stress lines. Therefore, the Manson-Haferd parameter, P_{MH}, determines two constants compared to the Larson-Miller parameter that involves only one constant. Rearranging Eq. (6) gives [14, 15]:

$$P_{MH} = f\,(\sigma) = (\log t - \log t_a)/(T - T_a) \qquad (7)$$

According to Manson and Haferd's suggestion, the parameter P_{MH} can, thus, be derived graphically from the intersection point of the extrapolated iso-stress lines when plotting $\log t_f$ against T. Moreover, plotting P_{MH} versus stress, σ, will force all creep data to collapse onto a single 'master curve'. The equation of this curve can then be determined by a curve fitting technique, which yields an equation relating time to a given percent creep, temperature and stress [15].

In agreement with Manson and Haferd, it was postulated elsewhere [14] that the parameter P_{MH} was derived from the approximately linear relationship found experimentally between $\log t_f$ and T as well as from the trend of the data that converge at a common point (T_a, t_a). This parameter, therefore, measures the slopes of the straight lines obtained for given values of stress. Values of T_a and $\log t_a$ which best fit the data vary for different materials [14]. Manson and Haferd showed that the values of T_a for most materials ranged from 0°F (−17.78°C) to 200°F (93.3°C) whereas the values of t_a varied appreciably [15]. Although single values of

T_a and log t_a might be found and universally agreed and used with satisfactory results, this possibility has not as yet been demonstrated. They also added that accurate results could be expected with this parameter, as with the LM parameter, only if the proper values of the constants were used for each material. However, the variation in the value of T_a and log t_a introduced many errors in extrapolating the short-term data, as it was found with the LM approach. Murray and Truman [16] also reviewed the MH technique and obtained new values of T_a and log t_a which accurately fitted the data of the austenitic steels used in the experiment. They also found that the values of the constants obtained were different from the standard values proposed by Manson and Haferd. Along with Murray and Truman, different values of these two constants were obtained elsewhere [17, 18] when experiments were carried out on different steels.

An advantage of the MH parameter is that it can be used for various materials and different times which could be either the time to a certain percent creep strain or the time to rupture. However, the numerical values of the MH constants read from the plots of log t_f against T are not precise enough unless very comprehensive experimental data are available. Furthermore, by using this technique, predicting the stress and the time values outside the temperature range on which the magnitudes of the constants are based can lead to significant errors [13]. An assessment carried out by Pink [19] stated that none of the methods had a consistent physical basis and that the apparent success of a certain procedure has only resulted from its applications in just circumstantial conditions. Furthermore, it was added that on one hand, the method of Larson and Miller, for instance, shows better consistency with the deformation processes occurring at low temperatures and thus, offers better results in the extrapolation of this type of data. Whereas on the other hand, the method of Manson and Haferd does not present any physical meaning, but coincidentally describes the complex pattern of deformation controlled by several mechanisms and is, thus, more reliable for long-term predictions of data generated at higher temperatures.

All of these methods were only proposed to analyse creep testing data since there is no mention in the literature of using the hot-tensile testing data, for example, in the analysis using these techniques [18]. Therefore, and based on these facts, the validity of this method is limited based on the conditions according to which the test is being carried out and thus, further research should be done in order to improve its capability of predicting the long-term creep properties before adopting its results.

2.4. Review of the Orr-Sherby-Dorn (OSD) methodology

The Orr-Sherby-Dorn (OSD) technique [20] involves a time-temperature parameter based on the parallelism of the iso-stress lines of a slope that represents the Orr-Sherby-Dorn constant, C_{OSD}. In this methodology, the assumptions of the Larson-Miller technique have been interchanged. In other words, the constant of the Larson-Miller equation, C_{LM}, became a function of stress whereas the parameter, P_{LM}, became a constant [2, 14]. Based on these new assumptions, the LM relation (Eq. (4)) can be re-arranged to give the OSD equation as [20]:

$$P_{OSD} = f(\sigma) = \log t_f - C_{OSD}/T \tag{8}$$

where P_{OSD} and C_{OSD} are the Orr-Sherby-Dorn parameter and constant, respectively, T is the absolute creep test temperature and t_f is the time to fracture. The basis of the OSD life prediction methodology is that the activation energy, Qc, remains constant over the entire creep curve, with relatively sparse supporting data [20]. However, since the constant C_{OSD} includes the activation energy, Qc, then any variations in Qc will, thus, ensure that the superimposed parametric plots will be non-linear [5, 6]. Indeed, there is evidence that in some cases, the creep activation energy seems to increase systematically through the primary region [21].

In order to prove the variation in the value of C_{OSD}, tests were carried out by Murray and Truman [16] and graphs of log t_f against 1/T at constant stress values were plotted. The gradients of these plots, that is, the values of C_{OSD}, were also calculated. Eventually, it was found that in spite of the difference between the values of C_{OSD} obtained experimentally and the values proposed by Orr, Sherby and Dorn, the data were fitted with reasonable accuracy [16]. Since the slope of the resulting log t_f against 1/T line will be the numerical value of C_{OSD}, it was proposed by Orr, Sherby and Dorn that the adjacent log σ/log t_f curves will be equidistant from each other along the time scale [13]. Therefore, in principle, only one line of log t_f against 1/T at a constant stress needs to be drawn in order to determine the value of the constant C_{OSD}, although in practice, the average slope of lines corresponding to different stress levels would be determined. However, it was found quite impracticable to obtain such lines and, in consequence, another method for determining the value of C_{OSD} has been employed elsewhere [13]. A paper published by Mullendore [22] revealed certain limitations in methods that employ only a single time-temperature parameter, as with the OSD method, and this became particularly obvious in cases where structural instabilities were involved. It was also added that due to the multiplicity of rate processes affecting the creep strength of complex alloys at high temperatures, it is absolutely impossible for a single parameter to describe precisely all creep properties involved. A review was also carried out on some high temperature alloys in which it was observed that the criterion of a constant slope of the lines specified by the ODS methodology was even less accurate than the assumption of the LM technique [22]. Another critical assessment documented in Murry [14] and carried out by Garofalo [8, 23] revealed that at each test temperature, a separate curve could have been found in relation to the initial stress, which represents the variations of this method as well as the other two methods of Larson-Miller and Manson-Haferd. This leads to the conclusion that the parameters studied were not only functions of stress, but also of other parameters involved in the process. Therefore, this method is found to be indirect and not taking sufficient account for longer tests [24]. According to Brozzo [25], a plot of the logarithm of the minimum creep rate against the reciprocal of the absolute temperature, at constant stresses, should give a series of straight lines. The same results should be obtained if the logarithm of the time to fracture is plotted against the same variable, since it is linearly related to the minimum creep rate. Therefore, it was possible to interpret the ODS and the LM parameters in terms of these plots. However, appreciable deviations from the claimed linearity were generally exhibited, except possibly for a limited range of temperatures. The reasons behind the failure of the rate-process equation in solving this problem can be readily recognised from the possibility of the metal, or the alloy, to deform according to various creep mechanisms accompanied by different activation energies and the likelihood of occurrence of some metallurgical changes during creep. Along with these

findings, direct evidence has been obtained by many investigators that metals and solid solution alloys can undergo a plastic deformation in different ways depending on the temperature and straining-rate conditions [25].

Therefore, based on these investigations, this methodology needs to include more materials and different processes in order to construct a complete and a comprehensive agreement about the value of its constants and the linearity of the plots that its equation implies.

2.5. Review of the Manson-Succop (MS) methodology

The Manson and Succop (MS) methodology [26] is identified by the analysis of the iso-stress lines in the plot of log t_f versus T. The Manson-Succop parameter, P_{MS}, was based on the parallelism of these lines of a slope that represents the Manson-Succop constant, C_{MS}, and is given by [26]:

$$P_{MS} = f(\sigma) = \log t_f + C_{MS}T \tag{9}$$

This method, in addition to other methods, was reviewed by Zharkova and Botvina [27] who confirmed that during long-term creep tests, fracture mechanisms changed according to the applied stress and the loading time. In this regard, they stated that fracture under high applied stresses was purely intergranular, under medium applied stresses it was also intergranular but resulted from wedge cracks formation and was also intergranular under low stresses but resulted from the formation and development of pores along grain boundaries. The change of fracture mechanisms was responsible for the appearance of the kink points in the long-term strength curves [27]. The known time-temperature parametric methods such as the Larson-Miller, Dorn, Manson-Succop, Manson-Haferd and many others, were based on relations with fixed values of constants in a wide range of temperatures and fracture durations which, in return, ignored the changes of fracture mechanisms and led to many errors and overestimations of the long-term creep life. For this reason, these methods are not necessarily reliable for creep life predictions [27].

2.6. Review of the Manson-Brown (MB) methodology

In general, as generated data do not necessarily show a linear trend in their behaviour, it is then necessary to use more complex functions to fit these data. The simplest function with an adjustable degree of curvature is the power function. Consequently, it is actually not surprising to find a generation of non-linear parameters containing the functional forms of the previous linear parameters raised to some power. The parameter which best illustrates this progression in complexity is the Manson-Brown parameter, P_{MB}, of the form [28, 29]:

$$P_{MB} = f(\sigma) = (\log t - \log t_a)/(T - T_a)^q \tag{10}$$

In this expression, there are three constants (t_a, T_a and the exponent q) which can be determined by a 'trial and error' graphical method. This equation represents the general form of the previously mentioned linear parameters such that, it represents [29]: (a) Manson-Haferd equation

when q = 1, (b) Larson-Miller equation when q = −1 and T_a = 0, (c) Orr-Sherby-Dorn equation when log t_a and $1/T_a$ are both taken to be arbitrarily very large numbers with the condition that T_a log t_a = Qc and (d) Manson-Succop equation when q = 1 and log t_a and T_a are both taken to be arbitrarily very large numbers such that log t_a/T_a = − C_{MS}. This generalised technique is very beneficial and much better than the individual proposed methods such that the data would dictate the specific form of the equation instead of trying to force any equation to fit the data. Later on, Manson along with Roberts and Mendelson proposed a generalised parameter of the form [30]:

$$P_{Manson} = f(\sigma) = \sigma^V (\log t - \log t_a)/(T - T_a)^q \qquad (11)$$

where v is an additional stress exponent constant. This equation presents a more generalised form of the previous methods where more linear parameters can be derived just with a slight change in the values of the constants involved. These generalised equations, that is, Eqs. (10) and (11), provide better techniques to predict the creep behaviour since they encompass most of the known parametric approaches under different test conditions.

2.7. Review of the Monkman-Grant (MG) methodology

The Monkman-Grant (MG) parametric method [8] uses the minimum strain rate, $\acute{\varepsilon}_{min}$, as a key variable to assess the time to fracture, t_f [31]. Monkman and Grant [8] noticed that the rupture time in the long-term creep tests could be related to the minimum strain rate by a power function of the form [8, 31]:

$$C_{MG} = \acute{\varepsilon}_{min} \, t_f \qquad (12)$$

where C_{MG} is the Monkman-Grant constant and m is the time to fracture exponent. This equation suggests that the mechanisms that control creep deformation and creep rupture are, to a great extent, the same [8]. The constant, C_{MG}, in this relation usually depends on temperature [31]. The practical advantage of the Monkman-Grant rule is that the minimum strain rate, $\acute{\varepsilon}_{min}$, can be measured early in a creep test which, in return, facilitates the prediction of the long-term time to fracture, t_f. In other words, if the value of C_{MG} is determined, which is possible from short-term tests, the lifetime of a long-term test can be predicted once the minimum strain rate has been reached and recorded [31]. On the other hand, another study which was carried out by Borisenko et al. [18] argued that the product of the minimum creep rate and the time to fracture is a constant value, C_{MG}, which is independent of stress and temperature. They also added that the value of this constant ranges between 0.03 and 0.3 for all materials and that the value of m should be 1.0, which eliminates the exponent from this equation. But later, and after some experiments that were carried out on tungsten, they found that the relation must be of the exponential form.

Another interpretation presented by Davies and Wilshire [32], which was based on experiments carried out on pure nickel, suggested that the constant, C_{MG}, was only independent of stress and temperature under high temperature creep conditions, that is, above $0.45T_m$, where T_m is the absolute melting temperature of a material, whereas higher values of this constant

were recorded at temperatures below $0.45T_m$. Moreover, they found that the value of the exponent m was not varying appreciably from unity and thus, can be ignored.

Baldan and Kaftelen [33] observed that proportionality was generally found between t_f and $\acute{\varepsilon}_{min}$ when the material was strained. This observation was based on the long-term creep tensile tests where it was found that the time to fracture was inversely proportional to the power function of the minimum creep rate for relatively simple alloys such as pure metals and single phase alloys. Their equation is given by [33]:

$$C_{MG} = \acute{\varepsilon}_{min}{}^m \, t_f \tag{13}$$

where the value of the exponent m ranged between ~0.8 and ~0.95. Besides, it was found that the value of the constant, C_{MG}, ranged from ~ 2 to ~ 15, depending on the material and the microstructural variables as this constant represents the contribution of the secondary creep strain to the total failure strain [33]. This equation was based on when the material was strained, cavities and cracks grew, linked-up and led, eventually, to an intergranular creep fracture. Assuming that creep fracture is actually controlled by the creep growth of cavities at grain boundaries, this result would then be consistent with the Monkman-Grant equation as, from the very beginning, the fracture process is always linked to the creep process [33].

Dobes and Milicka [34] argued that the value of C_{MG} and m changed according to the applied stress in contrast to the studies of Davies and Wilshire [32] and Chih-Kuang Lin [31] who previously found that the value of C_{MG} was dependent on stress and/or temperature. Therefore, Dobes and Milicka modified the Monkman-Grant relation into the form [34]:

$$C_{MG} \, \varepsilon_f = \acute{\varepsilon}_{min}{}^m \, t_f \tag{14}$$

where ε_f is the fracture strain recorded at t_f. This relation accounts for a possible stress dependence of the product $(\acute{\varepsilon}_{min}{}^m \, t_f)$ due to changes in the fracture strain, ε_f, according to the applied stress. However, this modification of the equation does not improve the prediction capability since, instead of only one long-term creep parameter, that is, t_f, their relationship requires also the knowledge of the second long-term parameter, that is, ε_f. This is actually impractical since having known the values of these two parameters eliminates, in return, the need for any predictions which is mainly the aim of such approaches [35].

Some other studies [36] added that if continuous nucleation occurs, a modelling of the fracture process might lead to the Monkman-Grant relationship provided that diffusive and plastic coupling of cavity growth and cavity interactions are considered. Besides, this relationship might offer the possibility of long-term extrapolation if the same creep-deformation mechanism operates during the whole creep life [37]. A research done by Menon [38] on silicon nitride examined the applicability of the Monkman-Grant relationship in predicting the stress rupture life. The data showed that the Monkman-Grant lines relating the rupture life to the minimum creep rate were stratified with respect to temperature. For this reason, a modification to the known expression of the Monkman-Grant equation was proposed to accommodate this temperature dependence. Following this modification, another generalised form of the equation was proposed by Evans [39] who stated that the standard Monkman-Grant relation

has the advantage of the easy estimate of the life of a material once the minimum creep rate is known. This ability of estimating the life of a material can be practically achieved by testing specimens at specified operating conditions until the minimum creep rate, which typically occurs well before the material's end-of-life, is reached and then, the test can be interrupted. This creep rate can then be used to predict the long-term creep life using the Monkman-Grant equation. However, one important disadvantage of using this relation to predict the creep life is that at operating conditions, it can still take tens of thousands of hours to reach the minimum creep rate and tests of this length are often not viable from the practical and the economical perspectives.

Therefore, although the Monkman-Grant relationship is applicable in some situations, there is still a disagreement about a few details such as the values of the constants used in this relationship and whether they are stress and/or temperature dependents and thus, more materials have to be tested and examined using this technique in order to generalise its use.

2.8. Review of the θ-projection methodology

The θ-projection method is one of the extrapolation methods which proved its applicability, in some situations, in predicting the creep life. It can be summarised in that creep curves under uniaxial constant stress are measured over a range of stresses and temperatures and their shapes are recorded. These shapes are then 'projected' to other stresses and temperatures at which full creep curves can be re-constructed. The required properties are then read off the constructed curves [1, 40]. Thus, the θ-projection concept, in its most general form, the 4-θ equation, describes the variation of creep strain, ε, with time, t, according to [41]:

$$\varepsilon = \theta_1 \left[1 - \exp\left(-\theta_2\, t\right) \right] - \theta_3 \left[1 - \exp\left(\theta_4\, t\right) \right] \tag{15}$$

where t and T are the time and temperature, respectively, θ_1 and θ_3 are scaling parameters defining the extent of the primary and tertiary stages with respect to strain, while θ_2 and θ_4 are rate parameters characterising the curvature of the primary and tertiary creep curves, respectively [42]. In this equation, the two terms on the right hand side describe the normal primary and tertiary components in which a deceleration in creep rate is observed during the primary stage whereas an acceleration is recorded during the tertiary stage [43, 44]. This method was extensively studied by Evans [41] who argued that this technique has an added advantage over the other traditional parametric procedures in that creep predictions are not only limited to the rupture time. However, it was found that the interpolation and/or the extrapolation of the θ-function, traditionally used by this method, was not really the best predictor of the long-term life as more accurate results were obtained using simpler functional forms. Moreover, this equation was quite poor in fitting the experimental creep curve at small strain values [41]. Deviations from the actual creep measurements were also found when this equation was used, particularly in the late tertiary stage, by Evans and Wilshire [44] who attributed these deviations to the intergranular cracks that present immediately prior to fracture.

Another study carried out by Evans [45] was in agreement with one done by Evans [41] in that the θ-projection method gave the poorest projections of creep properties at low strains.

Therefore, a modification to this equation has been suggested by Evans [45] in order to improve the fit of the experimental data at the very small strain values. This has been achieved by adding another two extra parameters to Eq. (2.20), which gave the (6-θ equation) as [45]:

$$\varepsilon = \theta_1 \left[1 - \exp\left(-\theta_2\, t\right) \right] - \theta_3 \left[1 - \exp\left(\theta_4\, t\right) \right] + \theta_5 \left[1 - \exp\left(-\theta_6\, t\right) \right] \qquad (16)$$

Now, in this equation, the first two right hand terms have the same physical meaning as in Eq. (15), whereas the third term describes the early primary creep behaviour that results from the initial sliding relaxation across grain boundaries [42]. According to Evans [41, 42, 45], this modified equation provided more precise results when it was used to fit experimental creep data, especially at the early stages of the primary creep. This was a result of the third term that has been added which took into account the effect of grain boundary relaxation during the primary creep that was completely neglected by Eq. (15).

In comparison to the previous parametric methods, the θ-projection method was considered to be more reliable and more accurate in estimating the long-term creep life and thus, it has been widely used and studied in an effort to prove its validity for a wider range of materials. However, further studies are still needed to assure that the errors encountered by the first proposed model of this equation are completely eliminated by the introduction of the modified version.

2.9. Review of the hyperbolic tangent methodology

This technique has been developed by Rolls-Royce plc in the 1990s for the purpose of creep lifing predictions. It implies that the highest stress that can be applied on a specified material at a certain creep temperature is the ultimate tensile strength of that material, σ_{TS}. The stress rupture behaviour is described by hyperbolic tangent curves over a wide range of temperatures, such that [46–48]:

$$\sigma = \sigma_{TS}/2 \left\{ 1 - \tanh\left[k \ln\left(t/t_i \right) \right] \right\} \qquad (17)$$

where k and t_i are fitting parameters that can be obtained by regression analysis using the actual experimental data at each temperature. Once the values of k and t_i are obtained, they can be inserted into Eq. (17) to produce the stress rupture predictive curves. Alternatively, using the creep strain values, another hyperbolic function is used to predict the rupture behaviour, such that [46–48]:

$$\sigma = S_i \left\{ 1 + \tanh\left[S_L \ln\left(\varepsilon/\varepsilon_i \right) \right] \right\} \qquad (18)$$

where in this equation, the ($\sigma_{TS}/2$) term of Eq. (18) has been eliminated and replaced by the parameter S_i whereas k, t and t_i have been replaced by S_L, ε and ε_i, respectively. Again, the values of these parameters can be obtained by regression analysis using the actual experimental data at each temperature. This method differs from the θ-projection method in that it does not try to fit the actual creep curves and then find an expression that relates the fitting constants with stress and temperature, but it represents the creep data at any temperature as a 3-D surface that combines stress, strain and time [47, 48]. This method provided a very good fit for the stress rupture and creep strain behaviour based on the time to fracture and creep strain measurements of many alloys. The only limitation is that inflexion points were found in

these predictive curves with no theoretical explanation. Interestingly, in the stress rupture curves, these inflexion points took place at around $0.5\sigma_{TS}$ at each temperature as a result of changing the pattern of stress rupture behaviour, which might be expected above and below σ_y (or σ_{TS}). Moreover, in the strain-dependent rupture curves, this inflexion point was found at around ε_i which has a physical significance as the strain value at the minimum creep rate point of a creep curve [48].

2.10. Review of the minimum commitment (MC) methodology

This method was proposed by Manson and Ensign [49] in an effort to give a larger flexibility to the parametric analysis of creep data. In addition, it was invented in order to combine all the conflicting approaches into a single equation that will have a sufficient generality. This method is given by [49, 50]:

$$\log t + A\,P\,\log t + P = G \tag{19}$$

where t is the time, A is a constant dependent on the metallurgical stability of the alloy, P is a variable equal to: $R_1 (T - T_{mid}) + R_2 (1/T - 1/T_{mid})$, G is a variable equal to: $(B + C \log \sigma + D \sigma + E \sigma^2)$, and B, C, D, E, R_1 and R_2 are regression coefficients and T_{mid} is the mid-value of the temperature range for which the data are to be analysed. In this equation, it is apparent that there are seven constants that need to be determined by regression analysis. It was also found that the more unstable the material, the higher the negative value of A required to fit the data [51]. As the constant A defines the metallurgical stability of the material, a negative value means that the material has the tendency to precipitate embrittling phases whereas a zero value would mean that the material is stable [52]. Unfortunately, the use of any value of A other than zero led to non-linear multiple regressions [52].

Among those who studied this methodology was Jow-Lian Ding [53] who found that the results of the regression analyses indicated that the Minimum Commitment model fit the data slightly better than the Larson-Miller model. The reason was that this model has five independent variables whereas the Larson-Miller model has only two. This method was also studied thoroughly by Goldhoff [54] in his attempts to find the optimum value of A. In this regard, he found that when formulating a model using this technique, the resulting equations were always non-linear since the values of A and P were unknown. It was also found that when fitting the short-term data, there was, relatively, insensitivity to the value of A which is not true for the long-term creep data predictions.

In order to establish a confidence in the use and, alternatively, to reflect problems of this procedure, it should be applied to an existing set of data as well as much sparser data and there should be immediate research into the development of stability factors to enhance the effectiveness of this extrapolation procedure [54].

2.11. Review of the Goldhoff-Sherby (GS) methodology

This methodology pre-supposed the convergence of the iso-stress lines to the point $(1/T_a, t_a)$ located just below the region of the experimental data. The general equation of this technique is given by [55]:

$$P_{GS} = f(\sigma) = (\log t - \log t_a)/(1/T - 1/T_a) \tag{20}$$

where t_a and T_a are the time and temperature constants, respectively. For the purpose of examining this equation, it was used to analyse the results of the experiments carried out by Sobrinho and Bueno [56] on steels where it was found that the worst results were obtained when the Goldhoff-Sherby equation was used to fit the data in all cases. Therefore, due to the very narrow use of this methodology in creep data predictions in addition to the fact that only few studies were carried out to examine the validity of this technique, more research should be completed before generalising the use of this technique in predicting the creep properties for long-term purposes.

2.12. Review of the Soviet methodology

This method can be described by two models, namely: Soviet model (1) and (2), given by [57]:

$$\textbf{Soviet Model (1): } \log t = a + b \log T + c \log \sigma + d/T + f \sigma/T \tag{21}$$

$$\textbf{Soviet Model (2): } \log t = a + b \log T + c \log \sigma/T + d \sigma/T + f/T \tag{22}$$

where a, b, c, d and f are constants to be determined. In studying these models, some observations were presented by Evans [57] who stated that Soviet model (1) was highly effective in modelling the rupture times presented to it for estimation purposes, but it was totally inadequate for predicting data points not used in its estimation. However, this inability to generalise, or the tendency to overfit the interpolative data set, is a characteristic of all parametric techniques [57].

2.13. Review of the Wilshire equations method

By using this new methodology, the values of the minimum creep rate, $\acute{\varepsilon}_m$, and the time to fracture, t_f, recorded at different temperatures can be superimposed onto 'Master Curves' by simply normalising the applied stress through the ultimate tensile strength, σ_{TS}, measured at various creep temperatures [5, 6]. Superimposition can also be achieved using the yield strength, σ_y, but the data fit is usually poorer since the value of σ_y is more difficult to be measured precisely than σ_{TS} [58]. Therefore, by selecting σ_{TS} values for such purposes, property comparisons for different metals and alloys can be significantly simplified [5, 6]. Normalising the applied stress in the power law equation, $\acute{\varepsilon}_m = A \sigma^n \exp(-Qc/RT)$, and defining the minimum creep rate, $\acute{\varepsilon}_m$, as in the Monkman-Grant relationship, $\acute{\varepsilon}_m = M/t_f$, gives [5, 6]:

$$\acute{\varepsilon}_m = M/t_f = A^* (\sigma/\sigma_{TS})^n \exp(-Qc^*/RT) \tag{23}$$

where $A^* \neq A$ and $Qc^* \neq Qc$. In this case, Qc^* is determined from the temperature dependence of $\acute{\varepsilon}_m$ and/or t_f at constant (σ/σ_{TS}), in contrast to Qc which is normally calculated at constant σ. Although this equation still does not permit reliable extrapolation of the short-term measurements as a result of the unpredictable fall in n values as σ/σ_{TS} decreases, it reduces, at least, the scale and the number of the experimental tests undertaken to obtain long-term strength data, but not the maximum duration of these tests [5, 6].

The failure of the traditional procedures to give acceptable estimates of the 100,000 h strengths by the analysis of the 30,000 h data has frequently been attributed to different mechanisms of creep and/or creep fracture which become dominant in different stress and temperature regimes [5, 6]. If the dominant mechanism changes, measurements made at high stresses would not allow prediction of the low-stress behaviour. For this reason, the new methodology has been introduced to examine and assess whether the change in the failure characteristics after prolonged creep exposure prevents accurate predictions of the long-term rupture strengths by extrapolating the short-term creep measurements [5, 6]. In this regard, Wilshire and Scharning [5, 6] obtained very accurate estimation of the long-term creep-rupture strength using this technique, irrespective of the transition from transgranular to intergranular fracture, by extrapolating the short-term creep data.

This technique is mainly based on the data rationalisation achieved through Eq. (23), where it is possible to rationalise the minimum creep rate, $\dot{\varepsilon}_m$, and the time to fracture, t_f, measurements by normalising σ through σ_{TS}. Since σ_{TS} represents the maximum stress that can be applied on a material at a specific creep temperature, the data sets can be described over the entire stress range from (σ/σ_{TS} = 1) to (σ/σ_{TS} = 0). In addition, it is evident that ($\dot{\varepsilon}_m \rightarrow \infty$ and $t_f \rightarrow 0$) as ($\sigma/\sigma_{TS} \rightarrow 1$), whereas ($\dot{\varepsilon}_m \rightarrow 0$ and $t_f \rightarrow \infty$) when ($\sigma/\sigma_{TS} \rightarrow 0$). These essential criteria are met by replacing Eq. (23), so that the stress and temperature dependences of the creep lives are described by [5, 6, 58]:

$$\sigma/\sigma_{TS} = \exp\left(-k_1 \left[t_f \exp(-Qc^*/RT)\right]^u\right) \tag{24}$$

where the values of the coefficients k_1 and u can be easily evaluated from the plots of $\ln [t_f \exp (- Qc^*/RT)]$ against $\ln [- \ln (\sigma/\sigma_{TS})]$. The slope of these plots represents the value of u whereas the intercept with the y-axis represents the value of $\ln (k_1)$ from which k_1 can be calculated. The value of Qc^* can be evaluated at constant σ/σ_{TS} by plotting $\ln (t_f)$ against $1/T$ where the slope of these plots represents the value of Qc^*/R from which Qc^* can be obtained. As with the representation of stress rupture properties through Eq. (24), the stress and temperature dependences of $\dot{\varepsilon}_m$ can be described using [5, 6, 58]:

$$\sigma/\sigma_{TS} = \exp\left(-k_2 \left[\dot{\varepsilon}_m \exp (Qc^*/RT)\right]^v\right) \tag{25}$$

where the values of the coefficients k_2 and v can be obtained from the plots of $\ln [\dot{\varepsilon}_m \exp(Qc^*/RT)]$ against $\ln [- \ln(\sigma/\sigma_{TS})]$. The slope of these plots represents the value of v whereas the intercept with the y-axis represents the value of $\ln (k_2)$ from which k_2 can be calculated. The value of Qc^* can be evaluated at constant σ/σ_{TS} by plotting $\ln (\dot{\varepsilon}_m)$ against $1/T$ where the slope of these plots represents the value of - Qc^*/R from which Qc^* can be obtained. In addition to Eqs. (24) and (25), the planned operational life for some components must take into account the times required to reach certain limiting strains, t_ε. As with t_f in Eq. (24) and $\dot{\varepsilon}_m$ in Eq. (25), the stress and temperature dependences of t_ε can be quantified as [5, 6]:

$$\sigma/\sigma_{TS} = \exp\left(-k_3 \left[t_\varepsilon \exp (-Qc^*/RT)\right]^w\right) \tag{26}$$

where the values of the coefficients k_3 and w can be calculated from the plots of $\ln [t_\varepsilon \exp (- Qc^*/RT)]$ against $\ln [-\ln (\sigma/\sigma_{TS})]$. The slope of these plots represents the value of w whereas

the intercept with the y-axis represents the value of ln (k_3) from which k_3 can be calculated. The value of Qc^* can be evaluated at constant σ/σ_{TS} by either plotting ln (t_f) and/or ln ($\acute{\varepsilon}_m$) against $1/T$ where the value of Qc^* can be obtained from the slope of these plots (the slope will be either Qc^*/R or $- Qc^*/R$, respectively). Studies by Wilshire and Scharning [5, 6, 59] revealed that using Eq. (24) allowed extrapolation of the short-term creep life measurements and accurately predicted the 100,000 h rupture strengths for several martensitic 9–12% chromium steels at different temperatures. Further studies by Wilshire and Scharning [5, 6] also showed that Eqs. (23)–(25) permitted effective rationalisation and extended extrapolation of the time to fracture, t_f, the minimum creep rate, $\acute{\varepsilon}_m$ and the time to certain strains, t_ε, data for 1Cr-1Mo-0.25 V steel, despite the tempering of the as received bainitic microstructure and the occurrence of a gradual transition from transgranular to intergranular fracture during creep exposure. In another study, Wilshire and Battenbough [58] proved that the stress and temperature dependences of $\acute{\varepsilon}_m$ and t_f were best described using Eqs. (24) and (25) when they used this technique on polycrystalline copper. Thus, using this new technique will certainly reduce the scale and duration of the test programmes currently undertaken to define the allowable creep strengths of power plants and aeroengine applications [59].

3. Analytical and modelling results

3.1. The Larson-Miller technique results

This technique has been investigated in order to find out whether the value of the constant, C_{LM}, used in its equation is actually a 'constant' or dependent on the test conditions. For this purpose, at constant stresses, $\log(t_f)$ was plotted against $1/T$ which gave straight lines of a slope equals to P_{LM} (the Larson-Miller parameter) and an intercept of - C_{LM} (the Larson-Miller Constant). The first observation that is in agreement with earlier studies [13, 14] was that even when these lines were extrapolated, they did not intersect at a certain point, which was assumed to represent the value of C_{LM}, as some studies [9] suggested. Besides, it is obvious from these plots that the value of C_{LM} is not constant (varied from ~ 14 to ~ 17). This analysis, therefore, suggests that the value of C_{LM} varies according to the test conditions, which agrees with previous studies [5, 6, 10, 14] and thus, disagrees with the assumption of the Larson-Miller technique [7]. However, as a first trial, an average value between 14 and 17 was used in order to obtain the stress rupture curves based on the Larson-Miller relation, but unfortunately, these curves did not fit the actual measurements accurately. The next attempt was to force all the creep data to collapse onto a single master curve by plotting the stress, σ, against the parameter P_{LM}, at randomly selected values of C_{LM}. The value of C_{LM} was considered only when it fitted the raw data perfectly based on the trial and error method. It was found that the best fit of the data was obtained when the value of C_{LM} was 20. From this plot, a relationship between the stress, time and temperature was obtained from which the stress-time predictive curves were constructed, **Figure 5**. The obtained curves were linear, equidistant and parallel. This implies that the relation between the stress and the time is, simply, linear which could lead, in return, to considerable errors as these curves did not fit the creep data accurately, especially at the higher stresses of each temperature, which agrees well with previous studies carried out on steels [12]. Actually, if fitting the creep data was that simple using a linear line,
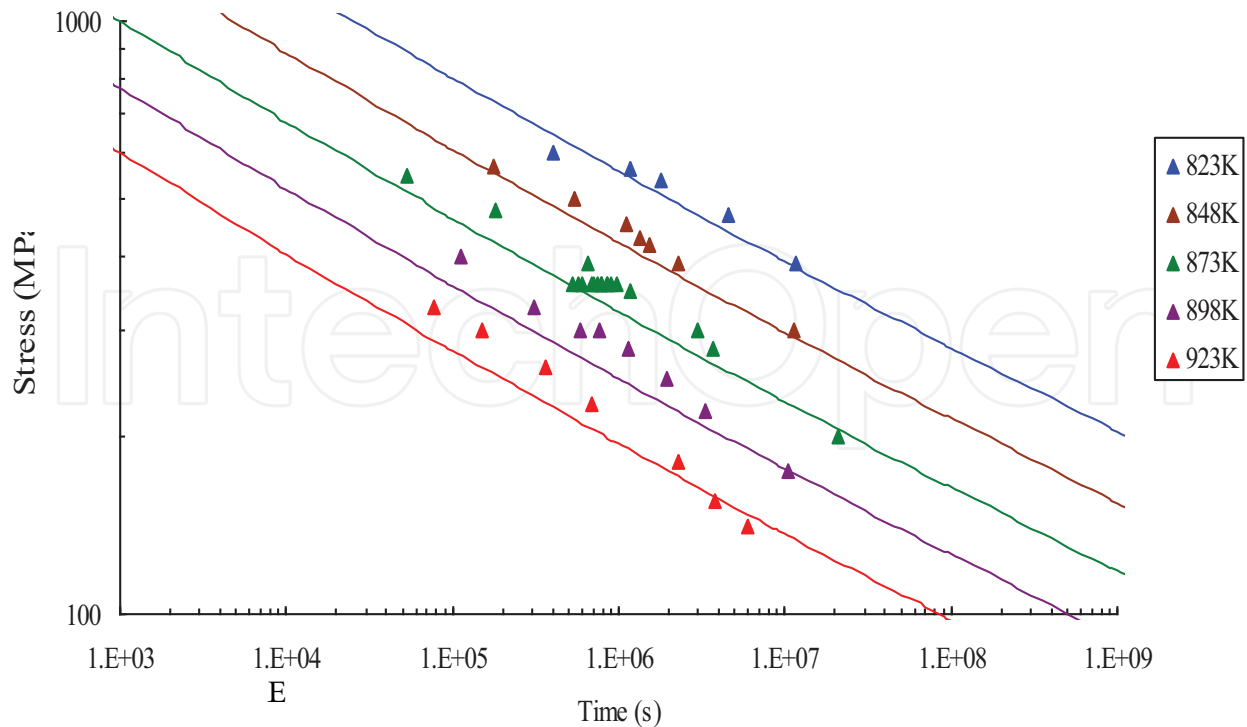
Figure 5. The Larson-Miller predictive curves.

there would not have been any need to develop complex relations to fit the data. But since the creep behaviour requires more complicated fitting equations to describe the actual creep behaviour, due to changes in creep mechanisms, linear relations will eventually lead to wrong estimations.

3.2. The Manson-Haferd technique results

As with all techniques, a relationship between the stress and the creep life at various temperatures is required. To start with the Manson-Haferd method, $\log(t_f)$ was plotted against T, at constant stresses, which gave straight linear lines of slope - P_{MH}, the Manson-Haferd parameter. When these lines were extrapolated, they did not meet at an intersection point of (T_a, t_a), as some studies [15] previously suggested. For this reason, another procedure was followed in order to calculate the values of these constants from the intersection point of the lines with the y and x-axes. The intercept of these linear lines represents the value of (P_{MH} T_a + $\log t_a$) from which the value of T_a and t_a can be calculated, sequentially. The average calculated values of T_a and $\log t_a$ for Titanium IMI834 were ~ 1061 and 29.713, respectively, which differ from the values suggested by Manson and Haferd and agree with other literature studies [16, 17, 56]. These values were then inserted into the Manson-Haferd equation and plotted against the stress, σ, at constant temperatures from which a relation between the stress and the Manson-Haferd parameter was obtained. This plot disagrees with some studies [15] which assumed that plotting this parameter against the stress superimposes all the data points into a single master curve. However, the predictive stress-time curves were obtained and plotted along with the actual creep results, **Figure 6**. The curves showed a better capability of fitting the
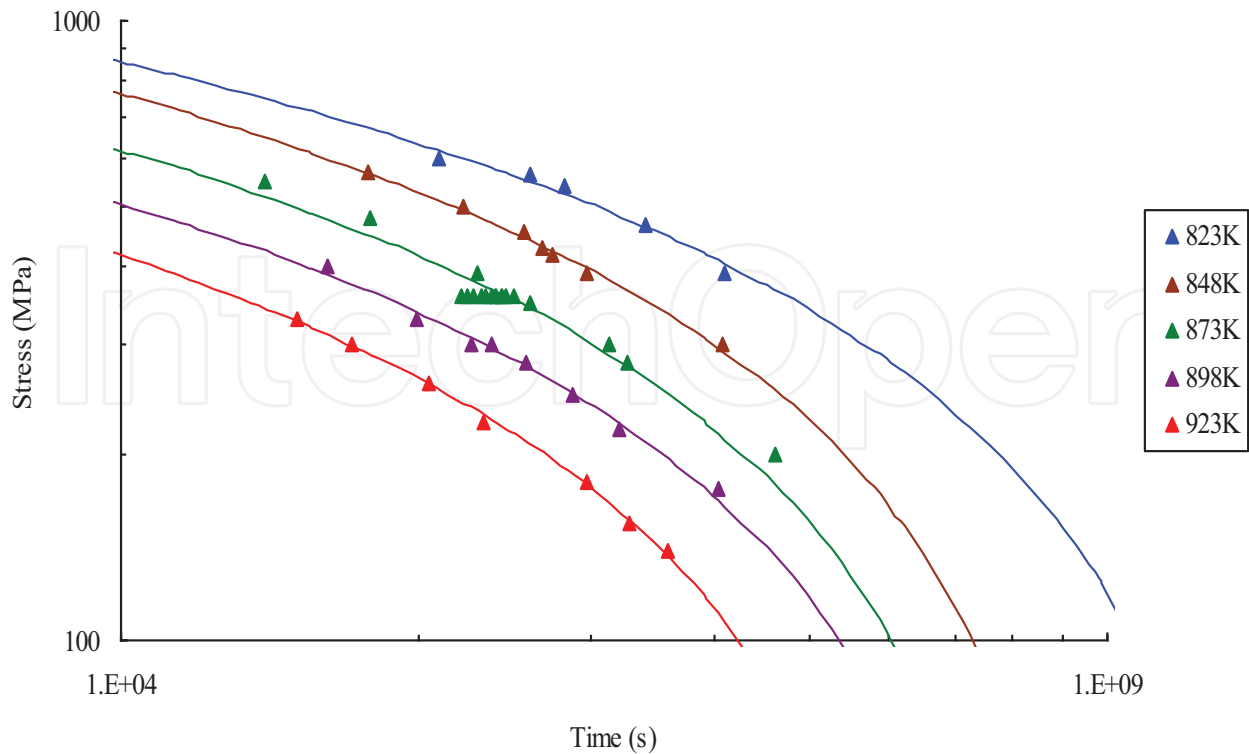
Figure 6. The Manson-Haferd predictive curves.

actual data points when compared with the Larson-Miller technique. This proves that the more complex the technique, the better its capability in predicting the creep properties.

3.3. The Orr-Sherby-Dorn technique results

The starting point of using this technique is similar to the Larson-Miller's analysis in which $\log(t_f)$ was plotted against $1/T$, at constant stresses. These plots gave straight lines of a slope which represents the value of C_{OSD}, the Orr-Sherby-Dorn constant, and an intercept with the y-axis equals to - P_{OSD}, the Orr-Sherby-Dorn parameter. The first result that can be drawn from these plots is that the value of C_{OSD} is not constant as the slope was changing from ~ 16,244 to ~ 20,053 with changing the stress and temperature. This outcome disagrees with the assumption of Orr, Sherby and Dorn [20] who assumed that the value of C_{OSD} is constant. As with the Larson-Miller technique, the same method employed there was used here to force all the data points to collapse onto a master curve by plotting the stress, σ, against the Orr-Sherby-Dorn parameter, P_{OSD}, with randomly selected values of C_{OSD}. The best fit of data was obtained when the value of C_{OSD} was ~ 20,000. This is consistent with the fact that this value lies in the range between 16,244 and 20,053, that is, the values of the slopes of the constant stress lines previously discussed. From this master curve, a relationship between the stress, time and temperature can be obtained from which the predictive stress-time curves can be constructed, **Figure 7**, at all temperatures. The curves fitted the actual creep data quite well where the curvature of these curves improved the fit. When compared with the Larson-Miller curves, **Figure 5**, it showed much better fit of the data at all temperatures and stresses. However, the Manson-Haferd curves, **Figure 6**, showed better consistency of the predictive curves with the actual data than the Orr-Sherby-Dorn curves,
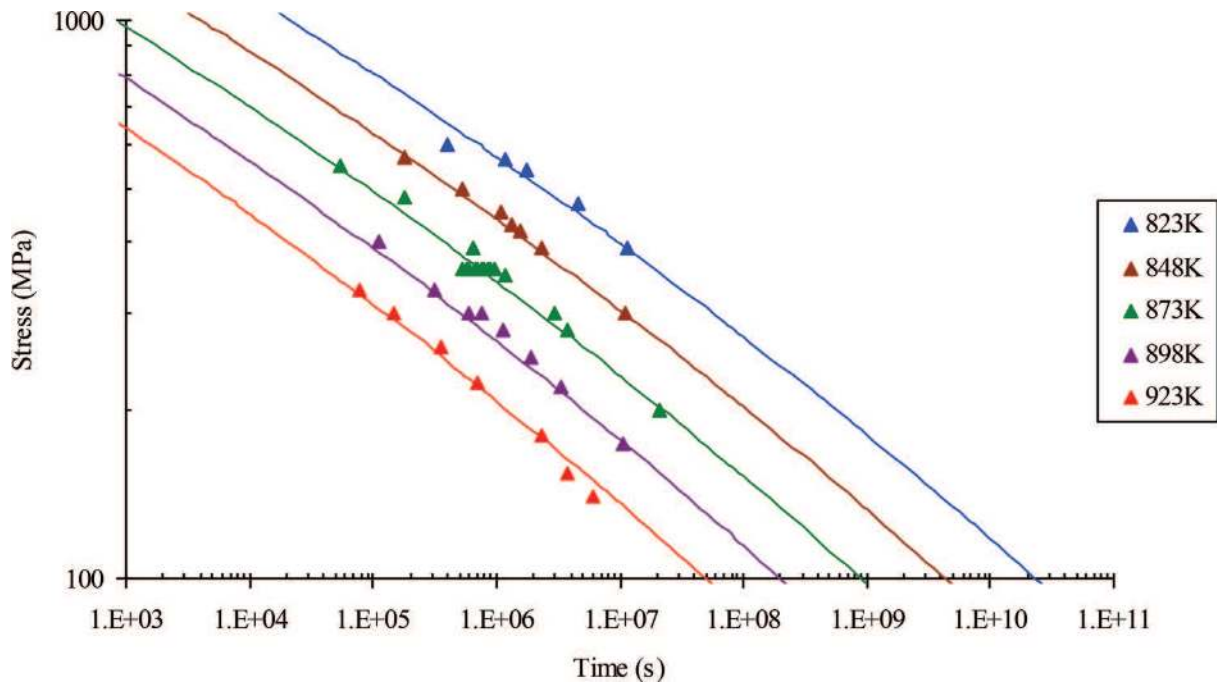
Figure 7. The Orr-Sherby-Dorn predictive curves.

Figure 7, as a higher degree of curvature was involved in the Manson-Haferd's curves as a result of the more complex function used in its equation.

3.4. The Manson-Succop technique results

The analysis using this technique started with plotting the values of $\log(t_f)$ against T, at constant stresses, which gave straight lines of slope equals to - C_{MS}, the Manson-Succop constant, and an intercept with the y-axis equals to P_{MS}, the Manson-Succop constant. These plots revealed that the slope, and hence the value of C_{MS}, varied between ~0.024 and 0.028 with varying the test conditions. This variation is relatively small but it could become more obvious if the tests conditions varied within a larger range of stresses and temperatures which might lead to a disagreement with the assumption of Manson and Succop [26] who confirmed that the value of C_{MS}, should be constant regardless of stress and temperature. However, an average value for C_{MS} was chosen, ~0.025, to superimpose all the data points onto a single curve by plotting the stress, σ, against the parameter, P_{MS}, from which a relation between the stress, time and temperature was obtained, **Figure 8**. This relation was then used to construct the stress-time curves on which the actual data points were projected, **Figure 8**. The stress-time curves were almost linear, equidistant and parallel (similar to the ones obtained using the Larson-Miller analysis). However, at the high temperatures (898 and 923 K), the fits were quite good in the high stress regime in comparison to the poor fits obtained in the low-stress regime. In contrast, the fits were quite good in the low-stress regime of the lower temperatures (823, 848 and 873 K), in comparison to the inferior fits obtained in high stress regime at these temperatures. Generally speaking, the fits were much better than those obtained from the Larson-Miller's analysis, but slightly less accurate than those obtained using the Manson-Haferd and Orr-Sherby-Dorn techniques.
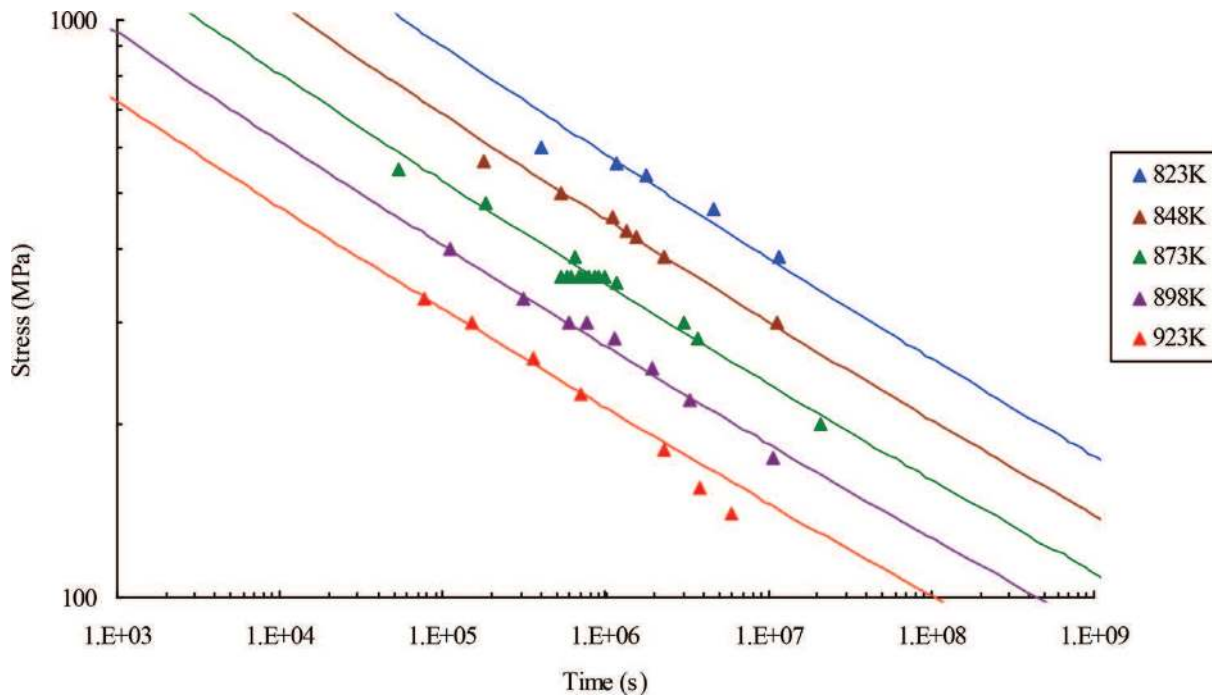
Figure 8. The Manson-Succop predictive curves.

3.5. The hyperbolic tangent technique results

For the purpose of finding the fitting parameters, plotting $\tanh^{-1}(1-2(\sigma/\sigma_{TS}))$ against $\ln(t_f)$, at constant temperatures, gave straight lines of a slope which represents the value of k and an intercept point with the y-axis equals to ($k \ln t_i$). From these plots, the values of the constant k and t_i were calculated at each corresponding temperature. These values were then inserted into the hyperbolic tangent equation from which the predictive stress-time curves were obtained, **Figure 9**. These curves showed an impressive fit of the actual creep data as a result of the complex functions used in this technique and thus, the smooth curvature which improved the fit. It can also be observed that there is an inflexion point at around 50% σ_{TS}, at each corresponding temperature, which agrees with other studies [46–48] and implies that the creep mechanism is dependent on the applied stress level. Another observation is that at the inter-mediate temperatures, that is, 848 and 873 K, the curves slightly deviated from the actual creep data trend at the stresses between ~300 and 500 MPa. Even though, this technique can be considered as an easy and a straightforward method which directly relates the stress to the time and temperature without the need to superimpose the data onto a master curve to obtain the stress as a function of these two parameters, as with the previous techniques. Moreover, the predictions are much better and more reliable than all of the previously obtained results of the other methods, as can be seen from the constructed plots.

3.6. The Goldhoff-Sherby technique results

This technique is very similar to the Manson-Haferd methodology concerning the procedure of analysing the Titanium IMI834 data with the only difference that $\log(t_f)$ is plotted against the reciprocal of T at constant stresses where the slope of the lines represents the value of the Goldhoff-Sherby parameter, P_{GS}. Moreover, this plot provides the value of the constants log
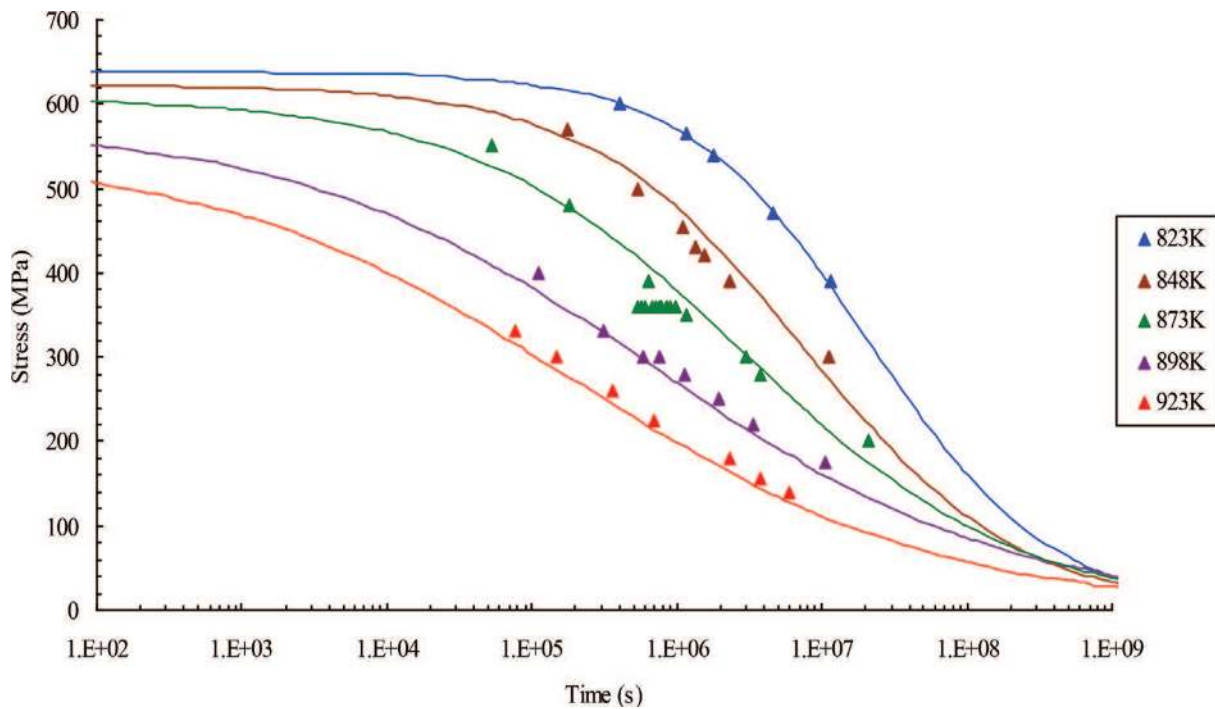
Figure 9. The hyperbolic tangent predictive curves.

t_a and $1/T_a$ from which a relationship between the stress and the Goldhoff-Sherby parameter, P_{GS}, can be obtained. For this purpose, an average value of log t_a and $1/T_a$ were taken as 15.824 and 0.0008, respectively. These relations between the stress and the parameter P_{GS} were then used in order to construct the stress rupture curves which showed a very good description of the actual creep results, **Figure 10**. The curves are very similar to those obtained by the Manson-Haferd technique which explains the similarity between these two methodologies in analysing the creep data. This again proves that the more complex the technique, the better its capability in predicting the long-term creep properties when compared to the simpler techniques.

3.7. The θ-projection technique results

Unlike the previously discussed models, this method was intended to fit the actual creep curves at various conditions and then express the fitting constants as functions of stress and temperature. The first version of this technique, the 4-θ was slightly able to fit the actual creep curves of Titanium IMI834. However, it did not give a very accurate description of the primary creep as many previous studies [41, 45] concluded, **Figure 11**. For this reason, the other version of this technique, the 6-θ, was used to fit the actual creep curves. Surprisingly, this equation provided a much better description of the primary creep behaviour which agreed very well with previous studies [41, 42, 45], **Figure 12**. This improvement in accurately fitting the primary creep confirms that the added two parameters, that is, θ_5 and θ_6, to the first version of this equation took into account the effect of grain boundary relaxation during the primary creep [42]. For both versions of the θ-method, the fitting procedure was possible by finding the values of the θ-parameters involved in their equation. The values of these parameters were
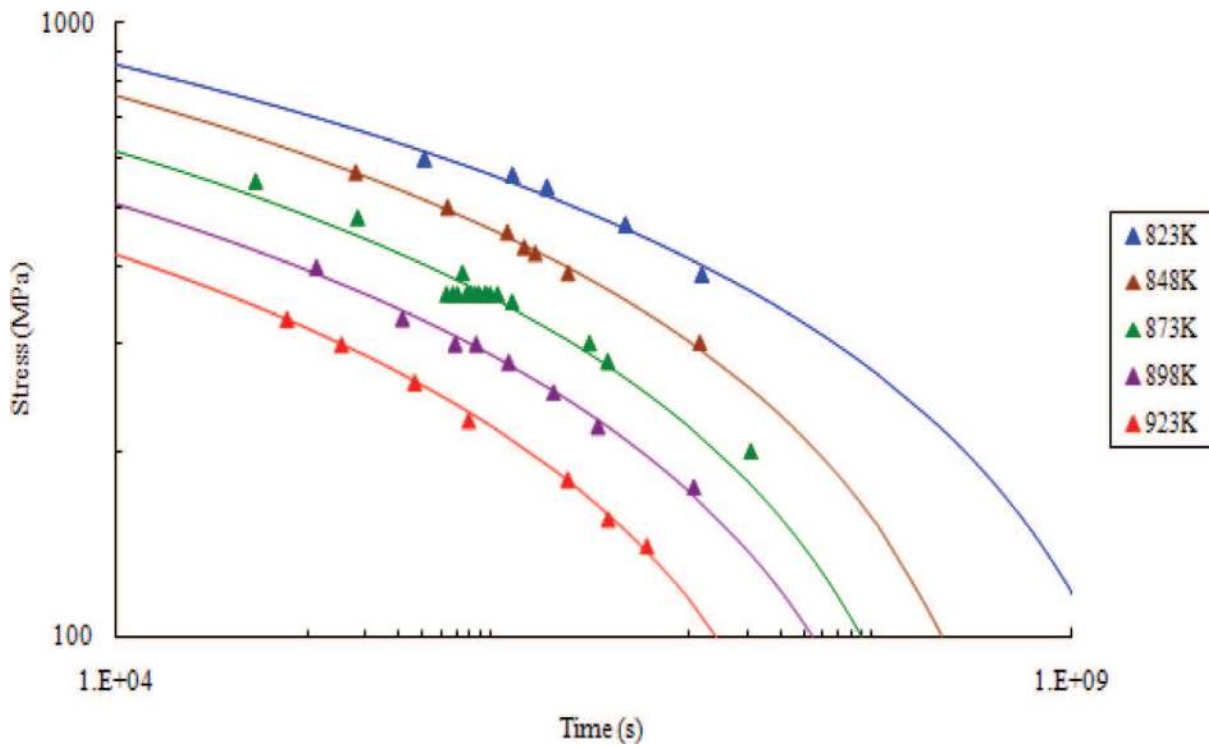
Figure 10. The Goldhoff-Sherby predictive curves.
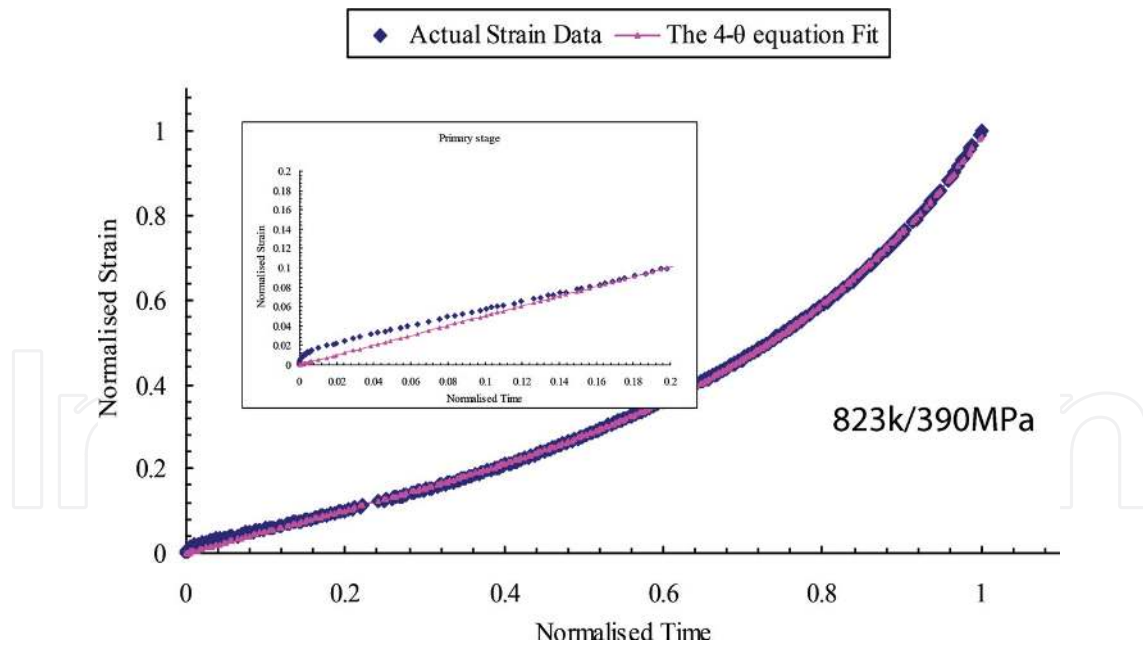

Figure 11. The fitting of the creep curve using the 4-θ method.

obtained by non-linear least square curve fitting routines (using SOLVER in Excel). Having obtained these parameters, many points and regions along the creep curve can then be defined, such as the primary and tertiary points, the minimum creep rate point, and the creep fracture, or the total ductility point. In these plots, the variation of each θ-term was plotted
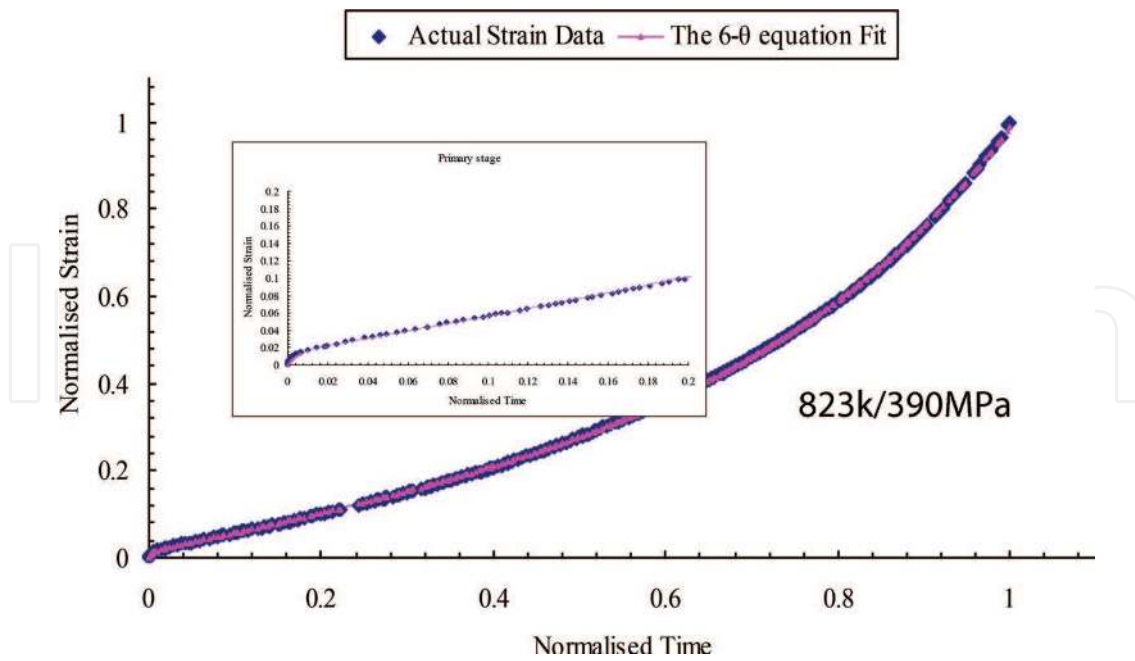
Figure 12. The fitting of the creep curve using the 4-θ method.

against stress at each individual temperature. The 4-θ results did not provide a systematic variation of the θ-parameters with stress for the primary creep region whereas the variation with the stress for the tertiary stage was slightly better, as it was found before [41]. This might be a result of the poor fit capability of this equation for the primary creep region. On the other hand, the 6-θ results provided a better description of all regions along the creep curve which is evident from the smooth and the linear variation with the stress. However, the trend of θ_3 and θ_5 was not purely linear, as they were, respectively, increasing/decreasing up to a certain stress level where they started to decrease/increase again at higher values of stress above that point. This unexpected change in the slope of these two parameters made it difficult to express them as a function of stress. If the trend of all parameters was completely linear, the values of these parameters could have been derived for any stress within the ranges studied experimentally. This means that this trend could have allowed interpolation of the data, although it might have also allowed reasonable extrapolation of creep properties. If the linear trends of the values of these parameters have been obtained, this means that they could have been expressed as functions of stresses and temperatures such that:

$$\theta = f(\sigma, T) \tag{27}$$

which means that Eqs. (15) and (16) could have been re-written as:

$$\varepsilon = f(t, \sigma, T) \tag{28}$$

In conclusion, this method requires the availability of full creep curves prior to using it as a predictive tool. This technique can be considered as a 'fitting' technique rather than a 'predictive' model as the stress-time curves cannot be derived from its equation.

3.8. The Wilshire technique results

In order to start the analysis using this technique, it was essential to find the value of the apparent activation energy, Qc^*, the tensile strength, σ_{TS}, at the applied temperatures and the values of the fitting parameters (k_1, k_2, k_3, u, v and w). Unlike the calculations of Qc, described in the power law equation, at constant σ, the value of Qc^* was determined at constant σ/σ_{TS} using the power law principle. This was possible by either plotting $\ln(t_f)$ or $\ln(\acute{\varepsilon}_m)$ against $1/T$ at constant σ/σ_{TS} where the slope of these plots represents the value of Qc^*/R and $-Qc^*/R$, respectively. From the plot of $\ln(t_f)$ against $1/T$, the value of Qc^* was ~305 kJ/mol whereas it was ~ 332 kJ/mol from the plots of $\ln(\acute{\varepsilon}_m)$ against $1/T$. The difference in the value of Qc^* using either of these two procedures was not too large and thus, an overall average value of 320 kJ/mol was used to run the analysis. It can be seen that this overall value of Qc^* is not far away from the value of Qc (~327–344 kJ/mol) calculated at constant σ. The values of the constants k_1 and u were determined by plotting $\ln(-\ln \sigma/\sigma_{TS})$ against $\ln(t_f \exp(- Qc^*/RT))$ where the slope of these plots provided the value of u whereas the intercept is the value of $\ln k_1$. However, it was observed that the linear trend of these plots deviated at a certain point that separated the data into two linear regimes, namely: the high- and the low-stress regimes. Based on this fact, different values of u and k1 were obtained from these two regimes. The predictive curves, **Figure 13**, showed a superb fit of the actual measurements in both the high and the low-stress regimes at all temperatures. It can be observed from these curves that there is a 'kink' point at which the trend of the creep data changed according to the stress level involved. This point exactly corresponds to the point found earlier in the plots of $\ln (-\ln \sigma/\sigma_{TS})$ against $\ln (t_f \exp(- Qc^*/RT))$ and this confirms that the dependence on stress level is more dominant than the temperature dependence, as the generated sigmoidal curve implied when
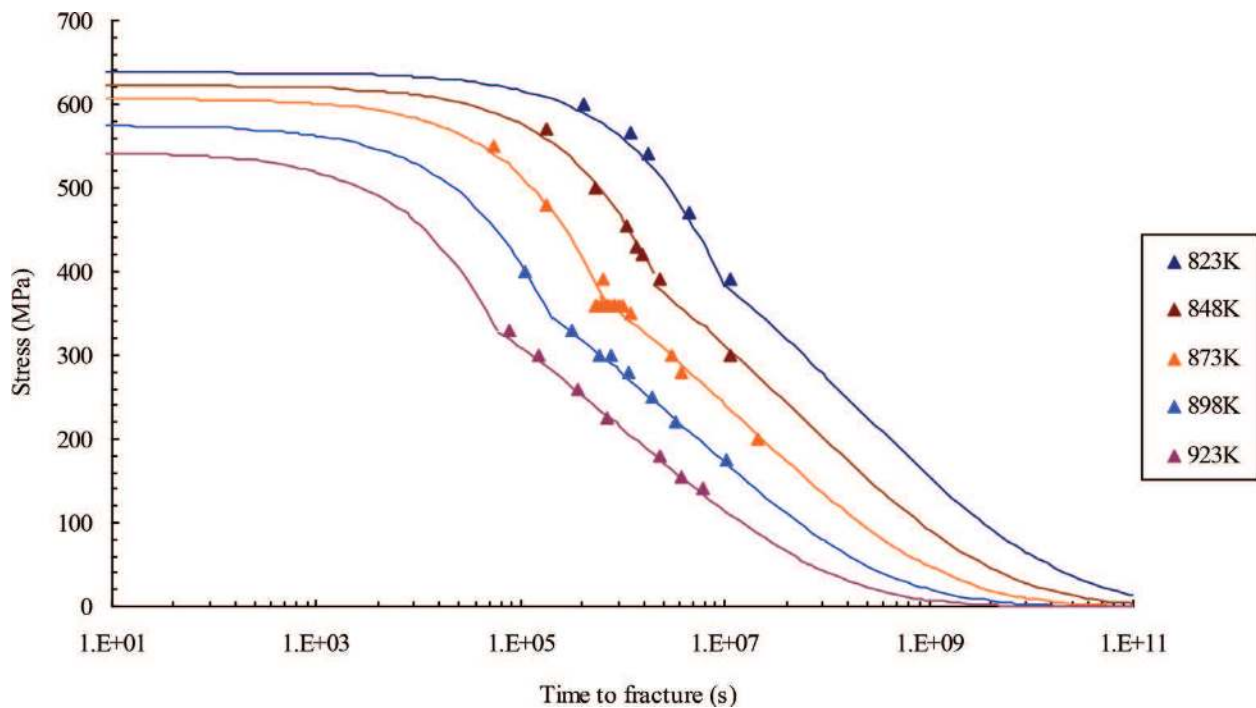

Figure 13. The Wilshire equations predictive curves.

the temperature dependence was eliminated. This predictability of the long-term creep behaviour using this equation proves that it is possible to extrapolate the short-term creep measurements at all test conditions.

Interestingly, the lines of the Wilshire 'kink' points and the yield stress regression line were linear, equidistant and parallel (slope ~ 0.6). Besides, the ratio of the stresses at the kink points was ~ 85% of the yield stress at each corresponding temperature. This implies that the inflexion points of the Wilshire curves are a result of the different deformation mechanisms above and below the material's yield point which play a key role in the creep behaviour. This physical explanation provides a possible reason for having two stress regimes and thus, the 'kink' in the predictive curves. It is worthwhile mentioning that the kink points were ~ 60% of the ultimate tensile strength, which is almost consistent with the hyperbolic tangent technique results, **Figure 9**, where the inflexion point of its curves was at ~50% of the ultimate tensile strength at each corresponding temperature.

It was found that the value of w and k_3 used in Eq. (26) is independent of stress and temperature at any selected strain level. This means that they can be expressed over a range of selected strains, such that:

$$w = f_1(\varepsilon) \tag{29}$$

and

$$k_3 = f_2(\varepsilon) \tag{30}$$

Inserting these two expressions into Eq. (26) gives:

$$\sigma/\sigma_{TS} = \exp\left(-f_2(\varepsilon)\left[t_\varepsilon \exp(-Qc^*/RT)\right]^{f_1(\varepsilon)}\right) \tag{31}$$

Rearranging this equation will provide an equation that relates the strain, ε, to stress, σ, and temperature, T, with time, t, such that:

$$\varepsilon = f(t, \sigma, T) \tag{32}$$

Obtaining Eq. (32) means that full creep curves at various stresses and temperatures can be re-produced based on the Wilshire equations technique. This was confirmed by the re-constructed creep curves obtained from the Titanium IMI834 data, **Figure 14**. These plots provided a full description of the creep curves at various conditions in addition to the very impressive description of the primary creep. The primary creep was described very well in mostly all cases of stresses and temperatures. The advantage of this capability can be summarised in that when the time required to reach a certain strain level is obtained from a creep curve, the stress-time curves for that strain level can be constructed based on this equation. Moreover, expressing w and k_3 as functions of strain can provide a description of the creep curves at any stress and temperature. Similarly, these equations present a way to define the end point of the creep curve. In other words, when the time to fracture is obtained from any creep curve, it can be used to construct the stress rupture curves based on this
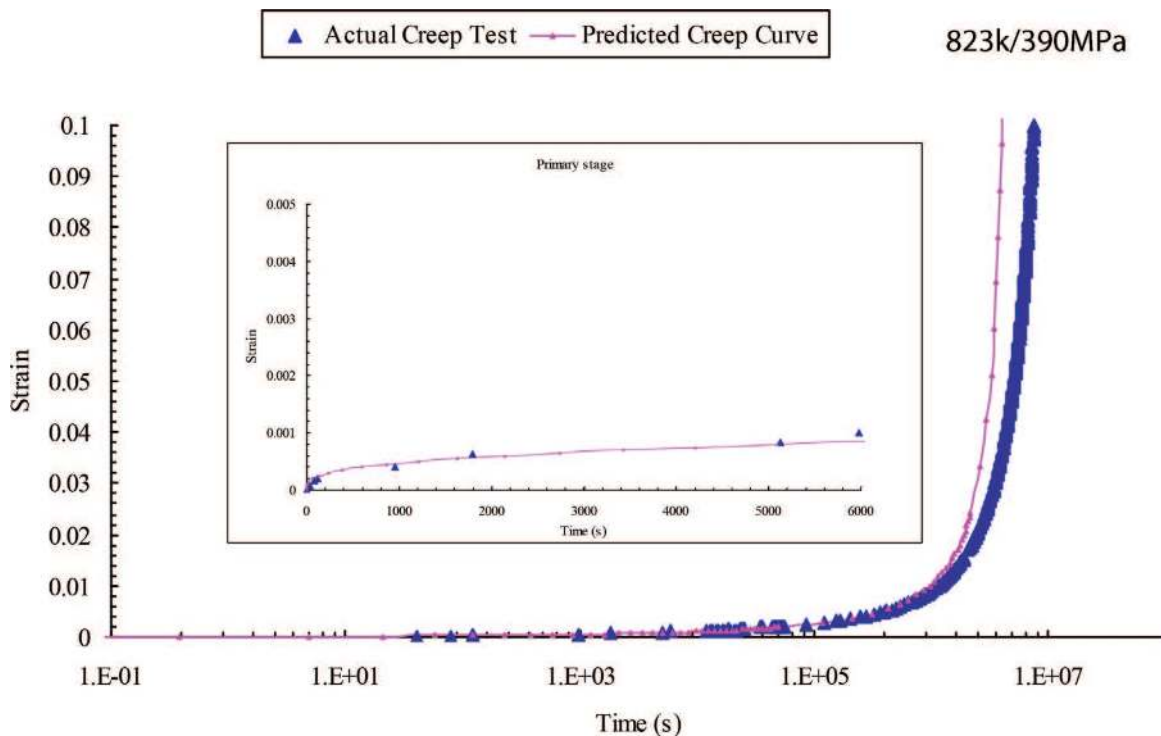
Figure 14. The re-produced creep curves using the Wilshire equations technique.

equation. In conclusion, in aerospace applications where the time to reach pre-defined strain levels is the main concern, typically ~1% strain level, then this technique provides an impressive description of the low strain levels required for such applications from the constructed creep curves.

4. Conclusions

- Using Titanium IMI834 data, it was revealed that the value of the stress exponent n and the activation energy Qc used in the power law equation are not constants which violates the original assumption of the power law which assumed that the value of these parameters is constant. This limits the use of this equation for long-term creep predictions. However, this equation can still be used as a mean to measure the value of the activation energy for different materials.

- When the Larson-Miller equation was examined using the Titanium IMI834, it was found that the value of the Larson-Miller constant CLM was actually not constant when the test conditions were altered. This disagrees with the assumption of Larson and Miller who assumed that the value of this 'constant' should be taken as 20 for all materials under all tests conditions. Moreover, the graphical method suggested by some scholars for obtaining the value of CLM was invalid for Titanium IMI834. Instead, an alternative procedure was used for determining the value of this constant. The stress rupture curves obtained from this equation were linear, equidistant and parallel. However, even with the

best chosen value of this constant, these curves did not fit the actual creep measurements accurately which led to overestimations of the long-term properties.

- The graphical method that was previously suggested by Manson and Haferd for determining the value of the constants Ta and ta was not applicable to Titanium IMI834. For this reason, another approach was used to find the values of these constants. Plotting the Manson-Haferd parameter PMH against the stress did not superimpose all the data points onto a single curve which violates the suggestions previously assumed by some researchers. The stress rupture curves showed a better consistency with the actual creep measurements when compared to the Larson and Miller curves. This capability of fitting the data points is a result of the more complex functions used in this equation in comparison to the Larson-Miller equation which suggests linear functions.

- The Orr-Sherby-Dorn equation was examined using the Titanium IMI834 creep data. The results showed that the constant used in their equation was not purely constant as it varied according to the applied test conditions. The stress rupture curves obtained fitted the actual creep data quite well and were more accurate than the Larson-Miller equation but less accurate than the Manson-Haferd relation.

- Applying the Titanium IMI834 data on the Manson-Succop equation revealed that the 'constant' used in their equation is actually not a constant and varied according to the test conditions which violates their assumption. Even when the best value of this 'constant' was used, the stress rupture curves were almost similar to those obtained from the Larson and Miller equation in that they were linear, equidistant and parallel. Despite this similarity, these curves fitted the actual measurements quite better than the Larson and Miller results. However, they were less accurate than the Manson-Haferd and the Orr-Sherby-Dorn equations.

- The hyperbolic tangent equation fitted the actual Titanium IMI834 creep measurements very well in comparison to all the previously used models. This equation is a straightforward and a more accurate procedure to be used for creep properties predictions. Interestingly, the inflexion points that can be observed in the stress rupture curves of this equation were found at ~50% of the ultimate tensile strength at each temperature. This means that the change in the long-term creep behaviour corresponds to the change in the applied stress level.

- The results of the 6-θ equation described the primary creep of Titanium IMI834 much more accurately when compared to the 4-θ equation at all test conditions. These two equations require full creep curves to be available in advance before they can be used in any application which makes them as 'fitting' equations rather than 'predictive' techniques. However, it was difficult to express the θ-parameters used in these equations as functions of stress which made it impossible to re-produce full creep curves based on these equations.

- The Wilshire equations showed a superb capability in fitting the actual measurements of Titanium IMI834. This was proved using the three forms of the Wilshire technique which accurately predicted the stress rupture, the minimum creep rate and the time to pre-defined strain values, respectively.

- In the Wilshire predictive curves, it was observed that there are inflexion, or 'kink', points at all temperatures. Investigations confirmed that these inflexion points took place at ~75% of the yield stress value at each corresponding temperature which split each curve into a high- and a low-stress regime. These points were also ~60% of the ultimate tensile stress which is almost consistent with the hyperbolic tangent equation results. This physical explanation implies that different deformation mechanisms are involved at each of these stress regimes.

- Full creep curves were re-constructed based on the Wilshire technique. This was possible by expressing the constants used in the Wilshire equation that predicts the time to reach certain strain levels as functions of strain, which was found to be impossible with the θ-technique. The re-constructed creep curves showed a very good description of the creep behaviour of Titanium IMI834 at all stresses and temperatures. The primary creep was also described very accurately, especially at the lower stress levels. This ability of re-producing the creep curves will, in return, save the time and cost required to carry out creep tests that might last for very long durations of time, especially at the lower stress levels.

Author details

Zakaria Abdallah*, Karen Perkins and Cris Arnold

*Address all correspondence to: Z.A.M.Abdallah@Swansea.ac.uk

Institute of Structural Materials, Swansea University, UK

References

[1] Wilshire B, Evans R. Introduction to Creep. London: The Institute of Materials; 1993

[2] Penny R, Marriott D. Design for Creep. 2nd ed. London: Chapman & Hall; 1995

[3] Cane B, Aplin P. Creep life assessment methods. The Journal of Strain Analysis for Engineering Design. Cane B & Aplin P, 1994. Creep life assessment methods. The Journal of Strain Analysis for Engineering Design. 1994;**29**(3):225-232

[4] Brown S, Evans R, Wilshire B. Creep strain and creep life prediction for the cast nickel-based Superalloy IN-100. Materials Science and Engineering. 1986;**84**:147-156

[5] Wilshire B, Scharning P. A new methodology for analysis of creep and creep fracture data for 9-12% chromium steels. International Materials Reviews. 2008;**53**(2):91-104

[6] Wilshire B, Scharning P. Prediction of long-term creep data for forged 1Cr-1Mo-0.25V steel. Materials Science and Technology. 2008;**24**(1):1-9

[7] Larson F, Miller J. A time-temperature relationship for rupture and creep stresses. Trans. ASME. 1952;**74**:223-249

[8] Monkman F, Grant N. An empirical relationship between rupture life and minimum creep rate in creep rupture tests. S.L. Proceedings ASTM. 1956;**56**:593-620

[9] Grote K, Antonsson E. Springer Handbook of Mechanical Engineering: Mechanical Properties. New York: Springer Science & Business Media; 2009

[10] Krivenyuk V, Mamuzic I. Correlation of creep-rupture data for complex alloys at elevated temperatures. Metalurgija. 2007;**46**(2):79-85

[11] Gilbert J, Long Z, Ningileri S. Application of Time-Temperature-Stress Parameters to High Temperature Performance of Aluminium Alloys. The Minerals, Metals & Materials Society, London, UK; 2007, 2007

[12] Cipolla L, Gabrel J. New Creep Rupture Assessment of Grade 91. University of Cambridge, Department of Materials Science and Metallurgy, Phase Transformations & Complex Properties Research Group, Cambridge, UK; 2005, 2005. Available at: https://www.phase-trans.msm.cam.ac.uk/2005/LINK/162.pdf

[13] Larke E, Inglis N. A critical examination of some methods of analysing and extrapolating stress-rupture data. s.l. Proceedings of the Institution of Mechanical Engineers. 1963

[14] Murry G. Extrapolation of the results of creep tests by means of parametric formulae. s.l. Proceedings of the Institution of Mechanical Engineers. 1963

[15] Manson S, Haferd A. A linear time-temperature relation for extrapolation of creep and stress-rupture data, s.l. In: NACA Technical Note 2890. 1953

[16] Murray J, Truman R. The high temperature properties of Cr-Ni-Nb and Cr-Ni-Mo austenitic steels. s.l. Proceedings of the Institution of Mechanical Engineers. 1963

[17] Bueno L, Sordi V, Marino L. Constant load creep data in air and vacuum on 2.25Cr-1Mo steel from 600°C to 700°C. Materials Research. 2005;**8**(4):401-408

[18] Sobrinho J, Bueno L. Correlation between creep and hot tensile behaviour for 2.25 Cr-1Mo steel from 500°C to 700°C. Part 2: An assessment according to different parameterization methodologies. Revista Matéria. 2012;**17**(3):1098-1108

[19] Pink E. Physical significance and reliability of Larson-Miller and Manson-Haferd parameters. Materials Science and Technology. 1994;**10**(4):340-346

[20] Orr R, Sherby O, Dorn J. Correlation of rupture data for metals at elevated temperatures. Trans. ASM. 1954;**46**

[21] Carreker R. Plastic flow of platinum wires. Journal of Applied Physics. 1950;**21**

[22] Mullendore A, Dhosi JW, Grant N. Study of parameter techniques for the extrapolation of creep rupture properties, in Conference Proceedings 1963. S.L. Proceedings of the Institution of Mechanical Engineers. 1963

[23] Garofalo F, Smith G, Royle B. Validity of time compensated temperature parameters for correlating creep and creep rupture data. Trans. Amer. Soc. Mech. Engs. 1956

[24] Allen N. The Extrapolation of Creep Tests, A Review of Recent Opinion. Institute of Metals, London, UK; 1960

[25] Brozzo P. A method for the extrapolation of creep and stress-rupture data of complex alloys. s.l. Proceedings of the Institution of Mechanical Engineers. 1963

[26] Manson S, Succop G. Stress-Rupture Properties of Inconel 700 and Correlation on the Basis of Several Time-Temperature Parameters. ASTM; 1956 Special Technical Publication (No. 174)

[27] Zharkova N, Botvina L. Estimate of the life of a material under creep conditions in the phase transition theory. Doklady Physics. 2003;**4**(7). (translated from Doklady Akademii Nauk, 2003. Volume: 391 (No. 3): p. 334-336. Original Russian Text Copyright)

[28] Manson S, Brown W. Time-temperature-stress relaxations for the correlation and extrapolation of stress-rupture data. s.l. Proceedings of the ASTM. 1953

[29] Viswanathan R. Damage Mechanisms and Life Assessment of High-Temperature Components. 2nd ed. Ohio: ASM International; 1993

[30] Manson S. Design consideration for long life at elevated temperatures. s.l. Proceedings of the Institution of Mechanical Engineers. 1963

[31] Lin C, Chu D. Creep rupture of lead-free Sn-3.5Ag and Sn-3.5Ag-0.5Cu solders. Journal of Materials Science: Materials in Electronics. 2005;**16**:355-365

[32] Davies P, Wilshire B. An Interpretation of the Relationship Between Creep and Fracture. s.l. The Iron and Steel Institute; 1960

[33] Baldan A, Kaftelen H. Comparative creep damage assessments using the various models. Journal of Materials Science. 2004;**39**(13):81-87

[34] Dobes F, Milicka K. The relation between minimum creep rate and time to fracture. Metal Science. 1976;**10**(11):382-384

[35] Dlouhy A, Kucharova K, Orlova A. Long-term creep and creep rupture characteristics of TiAl-base intermetallics, structural materials: Properties, microstructure and processing. Materials Science and Engineering A. 2009;**510/511**:350-355

[36] Davanas K, Solomon A. Theory of Intergranular creep cavity nucleation, growth and interaction. Acta Metallurgica. 1990;**38**(10):1905-1916

[37] Baldan A. Effects of carbides and cavitation on the Monkman-Grant ductility of a nickel-base superalloy. Journal of Materials Science Letters. 1992;**11**(19):1315-1318

[38] Menon M et al. Creep and stress rupture behaviour of an advanced silicon nitride: Part III, stress rupture and the Monkman-Grant relationship. Journal of the American Ceramic Society. 1994;**5**:77

[39] Evans M. A generalised Monkman-Grant relation for creep life prediction: An application to 1CrMoV rotor steel. Journal of Materials Science. 2006;**12**:41

[40] Tancret F, Sourmail T, Yescas M, Evans R. Design of a creep resistant nickel-base superalloy for power plant applications: Part 3 (experimental results). Materials Science and Technology. 2003;**19**

[41] Evans M. Sensitivity of the theta projection technique to the functional form of the theta interpolation/extrapolation function. Journal of Materials Science. 2002;**14**:37

[42] Evans R, Scharning P. The theta projection method applied to small strain creep of commercial aluminum alloy. Materials Science and Technology. 2001;**17**(5):31-45

[43] Evans R, Little E, Preston J, Wilshire B. 1993. Rationalisation of the creep behaviour of oxide-dispersion-strengthened alloys. s.l.. Fifth International Conference on Creep and Fracture of Engineering Materials and Structures

[44] Evans R, Wilshire B. The Role of Grain Boundary Cavities During Tertiary Creep. s.l. UK: Department of Metallurgy & Materials Technology, Swansea University; 2001. pp. 303-314

[45] Evans R. The theta projection method and low creep ductility materials. Materials Science and Technology. 2000;**16**(1):48-65

[46] Williams S. An Automatic Technique for the Analysis of Stress Rupture Data—Report MFR30017, s.l. Derby, UK: Rolls-Royce Plc; 1993

[47] Williams S. 1999. The implementation of creep data in component FE analysis. s.l. Compass 1999 Proceedings of the 1st International Conference on Component Optimisation, University of Wales, Swansea, United Kingdom

[48] Williams S, Bache M, Wilshire B. Recent developments in the analysis of high temperature creep and creep fracture behaviour. Materials Science and Technology. 2009

[49] Manson S, Ensign C. A Specialised Model for Analysis of Creep-Rupture Data by the Minimum Commitment, Station-Function Approach. s.l.: NASA TM-X-52999; 1971

[50] White W, May I, Silviera T. Design parameters for high temperature creep and the minimum-commitment method. Journal of Materials for Energy Systems. 1980;**2**(2):51-59

[51] Manson S, Ensign C. Interpolation and extrapolation of creep rupture data by the minimum commitment method, Part 1: Focal-point convergence. s.l. NASA TM-78881; 1978

[52] Park J, Manson S. A new approach for the characterisation of creep rupture properties for a newly fabricated material. s.l. The Sixth International Conference on Creep and Fatigue Design and Life Assessment at High Temperatures; 1996

[53] Ding J, Kenneth C, Brinkman C. A comparative study of existing and newly proposed models for creep deformation and life prediction of Si_3N_4. In: Life Prediction Methodologies and Data for Ceramic Materials. s.l.: s.n.; 1994. pp. 62-83

[54] Goldhoff R. Towards the standardisation of time-temperature parameter usage in elevated temperature data analysis. Journal of Testing and Evaluation, JTEVA 2. 1974;**5**:387-424

[55] Goldhoff R, Hahn G. Correlation and Extrapolation of Creep-Rupture Data of Several Steels and Superalloys Using Time-Temperature Parameters. Cleveland: American Society for Metals; 1968. ASM Publication D-8-100

[56] Sobrinho J, Bueno L. Correlation Between Creep and Hot Tensile Behaviour for 2.25 Cr-1Mo Steel from 500°C to 700°C. Part 2: An Assessment According to Different Parameterization Methodologies. s.l.: s.n; 2005

[57] Evans M. Method for improving parametric creep rupture life of 2.25Cr-1Mo steel using artificial neural networks. Materials Science and Technology. 1999;**15**:647-658

[58] Wilshire B, Battenbough A. Creep and creep fracture of polycrystalline copper. Materials Science and Engineering A. 2007;**443**:65-78

[59] Wilshire B, Scharning P. Long-term creep life prediction for a high chromium steel. Scripta Materialia. 2007;**56**:645-724